

Field theory of bicritical and tetracritical points. IV. Critical dynamics including reversible terms

R. Folk*

Institute for Theoretical Physics, Johannes Kepler University Linz, Altenbergerstrasse 69, A-4040 Linz, Austria

Yu. Holovatch†

*Institute for Condensed Matter Physics, National Academy of Sciences of Ukraine, 1 Svientsitskii Str., UA-79011 Lviv, Ukraine and
Institute for Theoretical Physics, Johannes Kepler University Linz, Altenbergerstrasse 69, A-4040 Linz, Austria*

G. Moser‡

*Department for Material Research and Physics, Paris Lodron University Salzburg, Hellbrunnerstrasse 34, A-5020 Salzburg, Austria
(Received 8 June 2011; published 24 February 2012)*

This article concludes a series of papers [Folk, Holovatch, and Moser, *Phys. Rev. E* **78**, 041124 (2008); **78**, 041125 (2008); **79**, 031109 (2009)] where the tools of the field theoretical renormalization group were employed to explain and quantitatively describe different types of static and dynamic behavior in the vicinity of multicritical points. Here we give the complete two-loop calculation and analysis of the dynamic renormalization-group flow equations at the multicritical point in anisotropic antiferromagnets in an external magnetic field. We find that the time scales of the order parameters characterizing the parallel and perpendicular ordering with respect to the external field scale in the same way. This holds independent whether the Heisenberg fixed point or the biconical fixed point in statics is the stable one. The nonasymptotic analysis of the dynamic flow equations shows that due to cancellation effects the critical behavior is described, in distances from the critical point accessible to experiments, by the critical behavior qualitatively found in one-loop order. Although one may conclude from the effective dynamic exponents (taking almost their one-loop values) that weak scaling for the order parameter components is valid, the flow of the time-scale ratios is quite different, and they do not reach their asymptotic values.

DOI: [10.1103/PhysRevE.85.021143](https://doi.org/10.1103/PhysRevE.85.021143)

PACS number(s): 05.50.+q, 64.60.Ht

I. INTRODUCTION

Three-component antiferromagnets in three spatial dimensions in an external magnetic field in z direction contain in their phase diagram two second-order transition lines: (1) between the paramagnetic and the spin flop phase and (2) between the antiferromagnetic and paramagnetic phase. The point where these two lines meet is a multicritical point, which turned out to be either bicritical or tetracritical. Within the renormalization group (RG) theory the stability and attraction region of the static fixed point (FP) of the RG transformation determines which kind of multicritical behavior is realized. For the bicritical point it is the Heisenberg FP; for the tetracritical point it is the biconical one. The stability of a FP depends on the system's global features as the space and order parameter (OP) dimensions d and n . In $d = 3$, the case considered here, the biconical FP is stable apart from a restricted attraction region of the Heisenberg FP. The static phase transition on each of the phase transition lines belongs for (1) to an isotropic Heisenberg model with $n_{\perp} = 2$ and for (2) to Heisenberg model with $n_{\parallel} = 1$ [1,2].

Concerning the dynamical universality classes the transition (1) belongs to the class described by model F, and (2) belongs to the model C class (for the notation see Ref. [3]). At the multicritical point the critical behavior is described by a new universality class in both statics and dynamics. The

interesting feature of these systems is that all the different OPs characterizing the ordered phase are physically accessible. This is most important for the dynamical behavior since the only other example belonging to model F is the superfluid transition in ^4He where the OP (the complex macroscopic wave function of the condensate [4]) is experimentally not accessible [5]. Here the OPs are the components of the staggered magnetization. Their correlations (static and dynamical) can be measured by neutron scattering.

A complete description of the critical dynamics near the multicritical point mentioned above has to take into account the slow dynamical densities, which are the OPs and the conserved densities present in the system. Due to the external magnetic field the only conserved density that has to be taken into account is the magnetization in the direction of the external field. A derivation of the dynamical equations follows along the usual steps calculating the reversible terms from the nonzero Poisson brackets, introducing irreversible terms present also in the hydrodynamic limit, dropping irrelevant terms and taking into account terms arising in the renormalization procedure (see, e.g., the review [3]). Such a dynamical model has already been considered in Refs. [6–8] by RG theory, and it was argued that due to nonanalytic terms in $\varepsilon = 4 - d$ a FP in two-loop order qualitative different from the one-loop FP is found. The result of the one-loop calculations is that the time scales of the parallel and perpendicular components of the staggered magnetization scale differently, whereas calculated in two-loop order they scale similar although the FP value of the time-scale ratio of the two components cannot be found by ε expansion and might be very small in $d = 3$, namely, of $O(10^{-86})$. It was argued that the terms leading to the singular

*folk@tphys.uni-linz.ac.at

†hol@icmp.lviv.ua

‡guenter.moser@sbg.ac.at

TABLE I. Dynamical FP values (zeros of the corresponding dynamical β functions) at $d = 3$ of different models for the time-scale ratios w_{\parallel}^* , w_{\perp}^* , v^* and the mode coupling constant f_{\perp}^* . The second and third lines quote results of this paper found in the biconical static FP for the tetracritical behavior of the dynamical model that takes into account reversible terms. They are compared with the two-loop results found in the model C multicritical point [11] as well as in the critical points of model C for the one component OP [9] and of model F for the two-component order parameter [10].

FP values in	w_{\parallel}^*	w_{\perp}^*	v^*	f_{\perp}^*
\mathcal{B}_C [11]	0.76	$\gg 1$	~ 0	—
\mathcal{B} one-loop	0	1.555	0	1.086
\mathcal{B} two-loop	0	0	~ 0	1.131
Model C [9]	0.49	—	—	—
Model F [10]	—	0	—	0.834

behavior in ε do not contribute to the FP value of the mode coupling. The calculations of the RG functions in Ref. [6] were not complete in two-loop order (they took into account only the terms that lead to the nonanalytic behavior in ε). At that time also the Heisenberg FP (named \mathcal{H}) was considered to be the stable static one, whereas it turned out in two-loop order (resummed) that it is the biconical FP (named \mathcal{B}) [2].

A summary of the results obtained so far for the FPs characterizing dynamical behavior is given in Table I. Neglecting the reversible terms one is left with a purely relaxational dynamics. Then the asymptotic dynamical critical behavior is characterized by the FP values of the independent time-scale ratios of the system. These are the time-scale ratios: (1) the ratio w_{\parallel} between the relaxation rate of the staggered magnetization parallel to the external field and the diffusive transport coefficient of the magnetization parallel to the external field; (2) the ratio w_{\perp} between the real part of the relaxation rate of the staggered magnetization perpendicular to the external field and the diffusive transport coefficient of the magnetization parallel to the external field. In addition we introduce the ratio v' between the two components of the real relaxation rates of the two OPs in order to compare their dynamic scaling behavior. A nonzero finite value of the time-scale ratio means that the two involved densities scale with the same exponent. If all time-scale ratios are nonzero and finite, one speaks of strong dynamic scaling, otherwise of weak dynamic scaling. Especially of interest is the behavior of the scaling of the two components of the OP indicated by the FP value of v' . In the third line of Table I the two-loop order result shows weak dynamic scaling between the OPs and the conserved density but strong scaling between the OP components. However, since the FP value of the time-scale ratio v' is almost zero, the critical behavior is dominated by nonasymptotic effects. For comparison the FP values for the case of model C for the one-component OP [9] and for model F for the two-component order parameter [10] are included. They are the limiting cases when the two OPs characterizing the multicritical behavior would decouple in statics and dynamics.

In the first line of Table I the results for the multicritical dynamical FP \mathcal{B}_C are displayed (see Ref. [11]), which take into account the static coupling of the OP to the conserved density. All time-scale ratios are nonzero and finite, but since

w_{\perp}^* is very large (v^* almost zero) the observable behavior in the vicinity of the multicritical point is predicted to be dominated by nonasymptotic effects, and strong scaling is not observable [11]. In the second line the results of a one-loop RG calculation with reversible terms for the biconical FP are given. The FP value of the mode coupling parameter f_{\perp} is finite, but since $w_{\parallel}^* = 0$ the critical dynamics is characterized by weak dynamic scaling, and the two components of the OP scale different. A similar result for the Heisenberg FP was found in Ref. [6]. In the third line the results found in this paper are shown, indicating weak scaling between the conserved density and the components of the OP, but strong scaling between the parallel and perpendicular components of the OP. Since the FP value of the time-scale ratio between the component v^* is almost zero but definitively different from zero, it is expected that nonasymptotic behavior is dominant.

This article concludes a series of papers [2,11,12] (henceforth cited as papers I, III, and II) where the tools of the field theoretical RG [13] were employed to explain and quantitatively describe different types of static and dynamic behavior in the vicinity of multicritical points. A short account of the results presented here was given in Ref. [14]. The statics and dynamics were treated in Refs. [2,11,12], respectively. First, purely relaxational dynamics was considered (paper II), and later, in paper III, these results served as a basis to consider how an account of magnetization conservation modifies dynamical behavior. The goal of the current study is more ambitious: We will analyze a complete set of dynamical equations of motion taking into account reversible terms [15,16] and give a comprehensive description of dynamical behavior in the vicinity of multicritical points in two-loop order. The paper is organized as follows: In Sec. II the dynamic model is defined followed by the definitions of the dynamical functions considered in Sec. III. The renormalization and corresponding RG functions are presented in Secs. IV and V, respectively. The two-loop results of our calculations for these dynamic RG functions are given in Sec. VI. The one-loop approximation for the dynamic is discussed in Sec. VII. In the Sec. VIII we consider the asymptotic properties of the two-loop RG functions leading to the general asymptotic results in Sec. IX. We then present the results expected in the asymptotic subspace in Sec. X. The nonasymptotic behavior, obtained by looking at the region farther away from the multicritical point, is shown in Sec. XI, and a conclusion (Sec. XII) ends the paper. In appendices calculational details for some intermediate steps of the RG calculation are presented.

II. MODEL EQUATIONS OF THE ANTIFERROMAGNET IN AN EXTERNAL FIELD

The nonconserved OP $\vec{\phi}_0$ of an isotropic antiferromagnet is given by the three-dimensional vector

$$\vec{\phi}_0 = \begin{pmatrix} \phi_0^x \\ \phi_0^y \\ \phi_0^z \end{pmatrix} \quad (1)$$

of the staggered magnetization, which is the difference of two sublattice magnetizations. An external magnetic field applied to the ferromagnet induces an anisotropy to the system. The

OP splits into two OPs, $\vec{\phi}_{\perp 0}$ perpendicular to the field, and $\vec{\phi}_{\parallel 0}$ parallel to the external field. Assuming the z axis in direction of the external magnetic field, the two OPs are

$$\vec{\phi}_{\perp 0} = \begin{pmatrix} \phi_0^x \\ \phi_0^y \end{pmatrix}, \quad \phi_{\parallel 0} = \phi_0^z. \quad (2)$$

In addition the z component of the magnetization m_0 has to be taken into account for the dynamics and therefore has to be included in statics, although there it could be integrated out and does not change the asymptotic static critical behavior. Thus the static critical behavior of the system is described by the functional

$$\begin{aligned} \mathcal{H} = \int d^d x \left\{ \frac{1}{2} \mathring{r}_{\perp} \vec{\phi}_{\perp 0} \cdot \vec{\phi}_{\perp 0} + \frac{1}{2} \sum_{i=1}^d (\nabla_i \vec{\phi}_{\perp 0}) \cdot (\nabla_i \vec{\phi}_{\perp 0}) \right. \\ \left. + \frac{1}{2} \mathring{r}_{\parallel} \phi_{\parallel 0} \phi_{\parallel 0} + \frac{1}{2} \sum_{i=1}^d (\nabla_i \phi_{\parallel 0}) (\nabla_i \phi_{\parallel 0}) + \frac{\mathring{u}_{\perp}}{4!} (\vec{\phi}_{\perp 0} \cdot \vec{\phi}_{\perp 0})^2 \right. \\ \left. + \frac{\mathring{u}_{\parallel}}{4!} (\phi_{\parallel 0} \phi_{\parallel 0})^2 + \frac{2\mathring{u}_{\times}}{4!} (\vec{\phi}_{\perp 0} \cdot \vec{\phi}_{\perp 0}) (\phi_{\parallel 0} \phi_{\parallel 0}) \right. \\ \left. + \frac{1}{2} m_0^2 + \frac{1}{2} \mathring{\gamma}_{\perp} m_0 \vec{\phi}_{\perp 0} \cdot \vec{\phi}_{\perp 0} + \frac{1}{2} \mathring{\gamma}_{\parallel} m_0 \phi_{\parallel 0} \phi_{\parallel 0} - \mathring{h} m_0 \right\}, \quad (3) \end{aligned}$$

with familiar notations for bare couplings $\{\mathring{u}, \mathring{\gamma}\}$, masses $\{\mathring{r}\}$, and field \mathring{h} [2,12]. The critical dynamics of relaxing OPs coupled to a diffusing secondary density is governed by the following equations of motion [6]:

$$\frac{\partial \phi_{\perp 0}^{\alpha}}{\partial t} = -\mathring{\Gamma}_{\perp}^{\alpha} \frac{\delta \mathcal{H}}{\delta \phi_{\perp 0}^{\alpha}} + \mathring{\Gamma}_{\perp}^{\alpha\beta z} \epsilon^{\alpha\beta z} \frac{\delta \mathcal{H}}{\delta \phi_{\perp 0}^{\beta}} + \mathring{g} \epsilon^{\alpha\beta z} \phi_{\perp 0}^{\beta} \frac{\delta \mathcal{H}}{\delta m_0} + \theta_{\phi_{\perp}^{\alpha}}, \quad (4)$$

$$\frac{\partial \phi_{\parallel 0}}{\partial t} = -\mathring{\Gamma}_{\parallel} \frac{\delta \mathcal{H}}{\delta \phi_{\parallel 0}} + \theta_{\phi_{\parallel}}, \quad (5)$$

$$\frac{\partial m_0}{\partial t} = \mathring{\lambda} \nabla^2 \frac{\delta \mathcal{H}}{\delta m_0} + \mathring{g} \epsilon^{\alpha\beta z} \phi_{\perp 0}^{\alpha} \frac{\delta \mathcal{H}}{\delta \phi_{\perp 0}^{\beta}} + \theta_m, \quad (6)$$

with the Levi-Civita symbol $\epsilon^{\alpha\beta z}$. Here $\alpha, \beta = x, y$, and the sum over repeated indices is implied.

The dynamical equations describe the dynamics of an antiferromagnet with the usual Lamor precession terms for the alternating magnetization and relaxation terms. Due to the static coupling to the conserved magnetization, additional Lamor terms arise together with a diffusive term for the magnetization. Renormalization considerations on the one hand lead to a neglecting of several Lamor terms and on the other hand create an additional reversible term (the second term on the right-hand side of Eq. (4)) not present in the usual dynamics of antiferromagnets [17].

Combining the kinetic coefficients of the OP to a complex quantity, $\mathring{\Gamma}_{\perp} = \mathring{\Gamma}_{\perp}^{\prime} + i\mathring{\Gamma}_{\perp}^{\prime\prime}$, the imaginary part constitutes a precession term created by the renormalization procedure even if it is absent in the background. The kinetic coefficient $\mathring{\lambda}$ and the mode coupling \mathring{g} are real. The stochastic forces $\theta_{\phi_{\perp}}$, $\theta_{\phi_{\parallel}}$,

and θ_m fulfill Einstein relations:

$$\langle \theta_{\phi_{\perp}}^{\alpha}(\vec{x}, t) \theta_{\phi_{\perp}}^{\beta}(\vec{x}', t') \rangle = 2\mathring{\Gamma}_{\perp}^{\alpha\beta} \delta(\vec{x} - \vec{x}') \delta(t - t') \delta^{\alpha\beta}, \quad (7)$$

$$\langle \theta_{\phi_{\parallel}}(\vec{x}, t) \theta_{\phi_{\parallel}}(\vec{x}', t') \rangle = 2\mathring{\Gamma}_{\parallel} \delta(\vec{x} - \vec{x}') \delta(t - t'), \quad (8)$$

$$\langle \theta_m(\vec{x}, t) \theta_m(\vec{x}', t') \rangle = -2\mathring{\lambda} \nabla^2 \delta(\vec{x} - \vec{x}') \delta(t - t'). \quad (9)$$

In view of dynamical calculations it is more convenient to deal with a scalar complex order parameter $\psi_0 = \psi_0' + i\psi_0''$ instead of the real two-dimensional OP $\vec{\phi}_{\perp 0}$ in Eq. (2). Thus we introduce

$$\psi_0 = \phi_0^x - i\phi_0^y, \quad \psi_0^+ = \phi_0^x + i\phi_0^y \quad (10)$$

as OPs of the perpendicular components. The superscript $+$ denotes complex conjugated quantities also in the following equations.

Expressed in terms of the complex OP the dynamic Eqs. (4)–(6) take the form

$$\frac{\partial \psi_0}{\partial t} = -2\mathring{\Gamma}_{\perp} \frac{\delta H}{\delta \psi_0^+} + i\psi_0 \mathring{g} \frac{\delta H}{\delta m_0} + \theta_{\psi}, \quad (11)$$

$$\frac{\partial \psi_0^+}{\partial t} = -2\mathring{\Gamma}_{\perp}^+ \frac{\delta H}{\delta \psi_0} - i\psi_0^+ \mathring{g} \frac{\delta H}{\delta m_0} + \theta_{\psi}^+, \quad (12)$$

$$\frac{\partial \phi_{\parallel 0}}{\partial t} = -\mathring{\Gamma}_{\parallel} \frac{\delta H}{\delta \phi_{\parallel 0}} + \theta_{\phi_{\parallel}}, \quad (13)$$

$$\frac{\partial m_0}{\partial t} = \mathring{\lambda} \nabla^2 \frac{\delta H}{\delta m_0} - 2\mathring{g} \text{Im}(\psi_0^+ \nabla^2 \psi_0) + \theta_m. \quad (14)$$

Due to the fact that the stochastic forces $\theta_{\phi_{\perp}}^{\alpha}$ in Eq. (4) are δ correlated and fulfill the Einstein relations, similar properties hold also for the stochastic forces θ_{ψ} :

$$\langle \theta_{\psi}(x, t) \theta_{\psi}^+(x', t') \rangle = 4\mathring{\Gamma}_{\perp}^{\prime} \delta(x - x') \delta(t - t'). \quad (15)$$

The critical behavior of the thermodynamic derivatives follows from the extended static functional (3) written in the densities introduced in Eq. (10). Then one has

$$\mathcal{H} = \mathcal{H}^{(0)} + \mathcal{H}^{(\text{int})} \quad (16)$$

with a Gaussian part

$$\begin{aligned} \mathcal{H}^{(0)} = \int d^d x \left\{ \frac{1}{2} \mathring{r}_{\perp} \psi_0^+ \psi_0 + \frac{1}{2} \sum_{i=1}^d (\nabla_i \psi_0^+) (\nabla_i \psi_0) \right. \\ \left. + \frac{1}{2} \mathring{r}_{\parallel} \phi_{\parallel 0}^2 + \frac{1}{2} \sum_{i=1}^d (\nabla_i \phi_{\parallel 0}) (\nabla_i \phi_{\parallel 0}) + \frac{1}{2} m_0^2 - \mathring{h} m_0 \right\}, \quad (17) \end{aligned}$$

and an interaction part

$$\begin{aligned} \mathcal{H}^{(\text{int})} = \int d^d x \left\{ \frac{\mathring{u}_{\perp}}{4!} (\psi_0^+ \psi_0)^2 + \frac{\mathring{u}_{\parallel}}{4!} \phi_{\parallel 0}^4 + \frac{2\mathring{u}_{\times}}{4!} \psi_0^+ \psi_0 \phi_{\parallel 0}^2 \right. \\ \left. + \frac{1}{2} \mathring{\gamma}_{\perp} m_0 \psi_0^+ \psi_0 + \frac{1}{2} \mathring{\gamma}_{\parallel} m_0 \phi_{\parallel 0}^2 \right\}. \quad (18) \end{aligned}$$

The above static functional may be reduced to the Ginzburg-Landau-Wilson (GLW) functional with complex OP by considering an appropriate Boltzmann distribution and integrating

out the secondary density. One obtains

$$\begin{aligned} \mathcal{H}_{\text{GLW}} = \int d^d x \left\{ \frac{1}{2} \hat{r}_\perp \psi_0^+ \psi_0 + \frac{1}{2} \sum_{i=1}^d (\nabla_i \psi_0^+) (\nabla_i \psi_0) \right. \\ \left. + \frac{1}{2} \hat{r}_\parallel \phi_{\parallel 0}^2 + \frac{1}{2} \sum_{i=1}^d (\nabla_i \phi_{\parallel 0}) (\nabla_i \phi_{\parallel 0}) + \frac{\hat{u}_\perp}{4!} (\psi_0^+ \psi_0)^2 \right. \\ \left. + \frac{\hat{u}_\parallel}{4!} \phi_{\parallel 0}^4 + \frac{2\hat{u}_\times}{4!} \psi_0^+ \psi_0 \phi_{\parallel 0}^2 \right\}. \end{aligned} \quad (19)$$

The parameters $\{\hat{r}\} \equiv \hat{r}_\perp, \hat{r}_\parallel$ and $\{\hat{u}\} \equiv \hat{u}_\perp, \hat{u}_\parallel, \hat{u}_\times$ in Eq. (19) are related to the corresponding parameters of the extended static functional (16) by

$$\hat{r}_\perp = \hat{r}_\perp + \hat{\gamma}_\perp \hat{h}, \quad \hat{u}_\perp = \hat{u}_\perp - 3\hat{\gamma}_\perp^2, \quad (20)$$

$$\hat{r}_\parallel = \hat{r}_\parallel + \hat{\gamma}_\parallel \hat{h}, \quad \hat{u}_\parallel = \hat{u}_\parallel - 3\hat{\gamma}_\parallel^2, \quad (21)$$

$$\hat{u}_\times = \hat{u}_\times - 3\hat{\gamma}_\perp \hat{\gamma}_\parallel. \quad (22)$$

The property that the static critical behavior does not depend on the secondary densities, which can be integrated out in Eq. (16), leads to relations between the correlation functions of the secondary densities and the OP correlation functions. These relations and their derivations have been extensively discussed in paper III with real OP functions $\phi_{\perp 0}$ and $\phi_{\parallel 0}$. Because the derivation of the relations is independent of the type of OP (real or complex), all of the relations remain valid and can be taken over from paper III. Therefore we will not repeat them here.

III. DYNAMIC CORRELATION AND VERTEX FUNCTIONS

The Fourier transformed dynamic correlation functions of the two OPs are usually introduced as

$$\hat{C}_{\psi\psi^+}(\{\xi\}, k, \omega) = \int d^d x \int dt e^{-ikx+i\omega t} \langle \psi_0(x, t) \psi_0^+(0, 0) \rangle_c, \quad (23)$$

$$\hat{C}_{\phi_\parallel \phi_\parallel}(\{\xi\}, k, \omega) = \int d^d x \int dt e^{-ikx+i\omega t} \langle \phi_{\parallel 0}(x, t) \phi_{\parallel 0}(0, 0) \rangle_c. \quad (24)$$

All functions depend on the two correlation lengths ξ_\perp and ξ_\parallel , which is indicated by $\{\xi\}$ in a short notation. $\langle AB \rangle_c = \langle AB \rangle - \langle A \rangle \langle B \rangle$ denotes the cumulant. The averages are calculated with a probability density including a dynamic functional, which can be constituted from the dynamic equations (11)–(14). In the considered approach of Ref. [18] for every density auxiliary densities are introduced accordingly. They are denoted as $\tilde{\psi}_0^+$, $\tilde{\psi}_0$, $\tilde{\phi}_{\parallel 0}$, and \tilde{m}_0 . The dynamic correlation functions of the order parameters are connected to dynamic vertex functions via

$$\hat{C}_{\psi\psi^+}(\{\xi\}, k, \omega) = -\frac{\hat{\Gamma}_{\tilde{\psi}\tilde{\psi}^+}(\{\xi\}, k, \omega)}{|\hat{\Gamma}_{\psi\psi^+}(\{\xi\}, k, \omega)|^2}, \quad (25)$$

$$\hat{C}_{\phi_\parallel \phi_\parallel}(\{\xi\}, k, \omega) = -\frac{\hat{\Gamma}_{\tilde{\phi}_\parallel \tilde{\phi}_\parallel}(\{\xi\}, k, \omega)}{|\hat{\Gamma}_{\phi_\parallel \phi_\parallel}(\{\xi\}, k, \omega)|^2}, \quad (26)$$

where the two-point vertex functions appearing on the right-hand side in the above expression have to be calculated within perturbation expansion. They are obtained by collecting all

one-particle irreducible Feynman graphs with corresponding external legs. A closer examination of the loop expansion reveals [19] that the dynamic response vertex functions $\hat{\Gamma}_{\psi\tilde{\psi}^+}$ and $\hat{\Gamma}_{\phi_\parallel \tilde{\phi}_\parallel}$ have the general structure

$$\begin{aligned} \hat{\Gamma}_{\psi\tilde{\psi}^+}(\{\xi\}, k, \omega) = -i\omega \hat{\Omega}_{\psi\tilde{\psi}^+}(\{\xi\}, k, \omega) \\ + \hat{\Gamma}_{\psi\psi^+}(\{\xi\}, k) \hat{\Gamma}_{\tilde{\psi}\tilde{\psi}^+}^{(d)}(\{\xi\}, k, \omega), \end{aligned} \quad (27)$$

$$\hat{\Gamma}_{\phi_\parallel \tilde{\phi}_\parallel}(\{\xi\}, k, \omega) = -i\omega \hat{\Omega}_{\phi_\parallel \tilde{\phi}_\parallel}(\{\xi\}, k, \omega) + \hat{\Gamma}_{\phi_\parallel \phi_\parallel}^{(d)}(\{\xi\}, k) \hat{\Gamma}_{\parallel}, \quad (28)$$

where $\hat{\Gamma}_{\psi\psi^+}(\{\xi\}, k)$ and $\hat{\Gamma}_{\phi_\parallel \phi_\parallel}(\{\xi\}, k)$ are the well-known static two-point vertex functions of the bicritical GLW model with a complex OP. We want to remark that the static vertex functions in Eqs. (27) and (28) are related by

$$\hat{\Gamma}_{\psi\psi^+}(\{\xi\}, k) = \frac{1}{2} \hat{\Gamma}_{\perp\perp}^{(2,0)}(\{\xi\}, k) \quad (29)$$

and

$$\hat{\Gamma}_{\phi_\parallel \phi_\parallel}(\{\xi\}, k) = \hat{\Gamma}_{\parallel\parallel}^{(2,0)}(\{\xi\}, k) \quad (30)$$

to the static vertex functions introduced in papers I–III for the model with real OPs. Thus the correlation lengths ξ_\perp and ξ_\parallel are now determined by

$$\xi_\perp^2(\{\hat{r}\}, \{\hat{u}\}) = \left. \frac{\partial \ln \hat{\Gamma}_{\psi\psi^+}(k, \{\hat{r}\}, \{\hat{u}\})}{\partial k^2} \right|_{k=0}, \quad (31)$$

$$\xi_\parallel^2(\{\hat{r}\}, \{\hat{u}\}) = \left. \frac{\partial \ln \hat{\Gamma}_{\phi_\parallel \phi_\parallel}(k, \{\hat{r}\}, \{\hat{u}\})}{\partial k^2} \right|_{k=0}. \quad (32)$$

$\hat{\Omega}_{\psi\tilde{\psi}^+}$, $\hat{\Gamma}_{\tilde{\psi}\tilde{\psi}^+}^{(d)}$, and $\hat{\Omega}_{\phi_\parallel \tilde{\phi}_\parallel}$ are purely dynamic functions. The explicit expressions of these functions are given in Appendix A, Eqs. (A1)–(A3). They determine also the dynamic vertex functions $\hat{\Gamma}_{\tilde{\psi}\tilde{\psi}^+}$ and $\hat{\Gamma}_{\tilde{\phi}_\parallel \tilde{\phi}_\parallel}$ in Eqs. (25) and (26). A proper rearrangement of the perturbative contributions shows that the relations

$$\hat{\Gamma}_{\tilde{\psi}\tilde{\psi}^+}(\{\xi\}, k, \omega) = -2 \text{Re}[\hat{\Omega}_{\psi\tilde{\psi}^+}(\{\xi\}, k, \omega) \hat{\Gamma}_{\psi\psi^+}^{(d)}(\{\xi\}, k, \omega)], \quad (33)$$

$$\hat{\Gamma}_{\tilde{\phi}_\parallel \tilde{\phi}_\parallel}(\{\xi\}, k, \omega) = -2\Gamma_\parallel \text{Re}[\hat{\Omega}_{\phi_\parallel \tilde{\phi}_\parallel}(\{\xi\}, k, \omega)] \quad (34)$$

hold. $\text{Re}[\cdot]$ is the real part of the expression in the brackets.

Analogous to (23) and (24) the Fourier transformed dynamic correlation function of the secondary density is introduced as

$$\hat{C}_{mm}(\{\xi\}, k, \omega) = \int d^d x \int dt e^{-ikx+i\omega t} \langle m_0(x, t) m_0(0, 0) \rangle_c \quad (35)$$

The connection to the dynamic vertex functions is analogous to the case of the OP [Eqs. (25) and (26)]:

$$\hat{C}_{mm}(\{\xi\}, k, \omega) = -\frac{\hat{\Gamma}_{\tilde{m}\tilde{m}}(\{\xi\}, k, \omega)}{|\hat{\Gamma}_{m\tilde{m}}(\{\xi\}, k, \omega)|^2}. \quad (36)$$

The dynamic response vertex function of the secondary density has the general structure

$$\begin{aligned} \hat{\Gamma}_{m\tilde{m}}(\{\xi\}, k, \omega) = -i\omega \hat{\Omega}_{m\tilde{m}}(\{\xi\}, k, \omega) \\ + \hat{\Gamma}_{mm}(\{\xi\}, k) \hat{\Gamma}_{\tilde{m}\tilde{m}}^{(d)}(\{\xi\}, k, \omega), \end{aligned} \quad (37)$$

where $\mathring{\Gamma}_{mm}(\{\xi\}, k)$ is the static two-point vertex function calculated with the extended static functional (16), which already has been introduced in paper III. A relation corresponding to (33) holds also for the dynamic vertex function of the secondary density. We have

$$\mathring{\Gamma}_{\tilde{m}\tilde{m}}(\{\xi\}, k, \omega) = -2 \operatorname{Re}[\mathring{\Omega}_{\tilde{m}\tilde{m}}(\{\xi\}, k, \omega) \mathring{\Gamma}_{\tilde{m}\tilde{m}}^{(d)}(\{\xi\}, k, \omega)]. \quad (38)$$

IV. RENORMALIZATION

A. Static renormalization

The renormalization of the GLW functional (19) has been extensively discussed in paper I. The only difference in the present paper is that we now have to renormalize the complex OP ψ_0 instead of the real vector OP $\vec{\phi}_{\perp 0}$. We introduce the following renormalization factor

$$\psi_0 = Z_{\psi}^{1/2} \psi, \quad \psi_0^+ = Z_{\psi}^{1/2} \psi^+, \quad (39)$$

where Z_{ψ} is a real quantity and identical to $Z_{\phi_{\perp}}$ in paper I taken at $n_{\perp} = 2$ and $n_{\parallel} = 1$. This means

$$Z_{\psi} = Z_{\phi_{\perp}} \Big|_{\substack{n_{\perp}=2 \\ n_{\parallel}=1}}. \quad (40)$$

The renormalization of the parameters $\hat{r}_{\perp}, \hat{r}_{\parallel}$ and the couplings $\hat{u}_{\perp}, \hat{u}_{\parallel}, \hat{u}_{\times}$ appearing in Eq. (19) is given in paper I [see Eqs. (16), (17), and (5)–(7)]. In all relations one has to replace $Z_{\phi_{\perp}}$ by Z_{ψ} . All renormalization factors remain valid if one sets $n_{\perp} = 2$ and $n_{\parallel} = 1$. This is also true for the Z matrix Z_{ϕ^2} introduced in Eq. (10) of paper I and the additive renormalization $A(\{u\})$ defined in Eq. (15) of paper I.

The renormalization of the parameters in the extended static functional (16) has been presented in paper III. As in the case of the bicritical GLW model all Z factors and relations between them remain valid if $Z_{\phi_{\perp}}$ therein is replaced by Z_{ψ} , and if one sets $n_{\perp} = 2$ and $n_{\parallel} = 1$ in explicit expressions.

B. Dynamic renormalization

Within dynamics auxiliary densities $\tilde{\psi}_0, \tilde{\phi}_{\parallel 0}$, and \tilde{m}_0 corresponding to the two OPs and the secondary density are introduced [18]. Instead of renormalization conditions we use the minimal subtraction scheme [20] as in the preceding papers II and III. The auxiliary density of the complex OP is multiplicatively renormalizable by introducing complex Z factors:

$$\tilde{\psi}_0 = Z_{\tilde{\psi}}^{1/2} \tilde{\psi}, \quad \tilde{\psi}_0^+ = Z_{\tilde{\psi}^+}^{1/2} \tilde{\psi}^+. \quad (41)$$

The complex renormalization factors in (41) fulfill the relation $Z_{\tilde{\psi}^+} = Z_{\tilde{\psi}}^+$. For the auxiliary densities of the single-component real OP and the secondary density the corresponding renormalization factors are introduced:

$$\tilde{\phi}_{\parallel 0} = Z_{\tilde{\phi}_{\parallel}}^{1/2} \tilde{\phi}_{\parallel}, \quad \tilde{m}_0 = Z_{\tilde{m}} \tilde{m}, \quad (42)$$

where $Z_{\tilde{\phi}_{\parallel}}$ and $Z_{\tilde{m}}$ are real. Within the minimal subtraction scheme the Z factors of the auxiliary densities of the nonconserved OPs $Z_{\tilde{\psi}^+}$ and $Z_{\tilde{\phi}_{\parallel}}$ are determined by the ε poles of the functions $\mathring{\Omega}_{\tilde{\psi}\tilde{\psi}^+}$ and $\mathring{\Omega}_{\tilde{\phi}_{\parallel}\tilde{\phi}_{\parallel}}$ introduced in Eqs. (27) and (28). The corresponding function of the conserved secondary

density $\mathring{\Omega}_{\tilde{m}\tilde{m}}$ in Eq. (37) does not contain new poles. Therefore one has

$$Z_{\tilde{m}} = Z_m^{-1}, \quad (43)$$

where Z_m has been introduced in Eq. (30) in paper III.

The kinetic coefficients renormalize as

$$\mathring{\Gamma}_{\perp} = Z_{\Gamma_{\perp}} \Gamma_{\perp}, \quad \mathring{\Gamma}_{\parallel} = Z_{\Gamma_{\parallel}} \Gamma_{\parallel}, \quad \mathring{\lambda} = Z_{\lambda} \lambda. \quad (44)$$

The renormalization of the complex kinetic coefficient Γ_{\perp} in Eq. (44) leads to a complex $Z_{\Gamma_{\perp}}$, while the other two renormalization factors in Eq. (44) are real valued. $Z_{\Gamma_{\perp}}$ can be separated into

$$Z_{\Gamma_{\perp}} = Z_{\psi}^{1/2} Z_{\tilde{\psi}^+}^{-1/2} Z_{\Gamma_{\perp}}^{(d)}, \quad (45)$$

where $Z_{\Gamma_{\perp}}^{(d)}$ contains the singular contributions of the dynamic function $\mathring{\Gamma}_{\psi\tilde{\psi}^+}^{(d)}$, appearing in Eq. (27).

The dynamic equation (13) for the OP ϕ_{\parallel} contains no mode coupling term. As a consequence only the kinetic coefficient $\mathring{\Gamma}_{\parallel}$ appears in the dynamic vertex function (28) instead of a function $\mathring{\Gamma}_{\phi_{\parallel}\tilde{\phi}_{\parallel}}^{(d)}$. Therefore $Z_{\Gamma_{\parallel}}^{(d)} = 1$, and we can write

$$Z_{\Gamma_{\parallel}} = Z_{\phi_{\parallel}}^{1/2} Z_{\tilde{\phi}_{\parallel}}^{-1/2}. \quad (46)$$

Using Eq. (43) the kinetic coefficient of the secondary density renormalizes as

$$Z_{\lambda} = Z_m^2 Z_{\lambda}^{(d)}, \quad (47)$$

where $Z_{\lambda}^{(d)}$ contains only the poles of the k^2 derivative of $\mathring{\Gamma}_{\tilde{m}\tilde{m}}^{(d)}$ taken at zero frequency and wave vector modulus.

The mode coupling coefficient needs no independent renormalization, so we simply have

$$\mathring{g} = \kappa^{\varepsilon/2} Z_m g A_d^{-1/2}. \quad (48)$$

The geometric factor A_d [21] already used in the static renormalization has been given in paper I [Eq. (8)].

V. RENORMALIZATION GROUP FUNCTIONS

In order to obtain the temperature dependence of the model parameters, as well as the asymptotic dynamic exponents, the RG functions, which are usually denoted as ζ and β functions, have to be introduced.

A. General definitions

In order to simplify the general handling of the RG functions we will use the uniform definition

$$\zeta_{\alpha_i}(\{\alpha_j\}) = \frac{d \ln Z_{\alpha_i}^{-1}(\{\alpha_j\})}{d \ln \kappa} \quad (49)$$

for all ζ functions in statics and dynamics. The derivative is taken at fixed bare parameters. $\{\alpha_j\}$ denotes the set of static and dynamic model parameters, which include the static couplings $\{u\}$ and $\{\gamma\}$, the mode coupling g , and all kinetic coefficients $\Gamma_{\perp}, \Gamma_{\perp}^+, \Gamma_{\parallel}, \lambda$. The ζ function ζ_{α_i} is calculated from the renormalization factor Z_{α_i} introduced in the previous section. Thus α_i may denote a model parameter from the set $\{\alpha_j\}$, a density $\psi, \phi_{\parallel}, m$, or a composite operator $\psi^2, \phi_{\parallel}^2$. The approach of the model parameters $\alpha_i(l)$ to their FP values in

the vicinity of the multicritical point is determined by the flow equations with the flow parameter l

$$l \frac{d\alpha_i(l)}{dl} = \beta_{\alpha_i}(\{\alpha_j(l)\}) \quad (50)$$

with β functions

$$\beta_{\alpha_i}(\{\alpha_j(l)\}) = \alpha_i(l)[-c_i + \zeta_{\alpha_i}(\{\alpha_j(l)\})]; \quad (51)$$

c_i is the naive dimension of the corresponding parameter α_i obtained by power counting. For the static couplings u_{\perp} , u_{\times} , or u_{\parallel} the naive dimension c_i is equal to ε , while for γ_{\perp} or γ_{\parallel} and the mode coupling g it is $\varepsilon/2$, respectively. All kinetic coefficients, these are Γ_{\perp} , Γ_{\perp}^+ , Γ_{\parallel} , and λ , are dimensionless quantities, which means $c_i = 0$.

The flow equations (50) have fixed points at the zeros of the β functions. The FP values of the model parameters $\{\alpha_j^*\}$ are defined by the equations

$$\beta_{\alpha_i}(\{\alpha_j^*\}) = 0. \quad (52)$$

The FP is stable if all eigenvalues of the matrix $\partial\beta_{\alpha_i}/\partial\alpha_k$ are positive or possesses positive real parts. Starting at values $\{\alpha_j(l_0)\}$ at an initial flow parameter value l_0 , the flow equations can be solved numerically. The asymptotic critical values of the parameters are obtained in the limit $l \rightarrow 0$. If a stable FP is present, the flow of the parameters has the property

$$\lim_{l \rightarrow 0} \{\alpha_j(l)\} = \{\alpha_j^*\}. \quad (53)$$

A set of FP values $\{\alpha_j^*\}$ determines all static and dynamic exponents. The static relations between ζ functions and critical exponents have been extensively discussed in papers I and III. The dynamic exponents are related by

$$z_{\phi_{\perp}} = 2 + \zeta_{\Gamma_{\perp}}^*, \quad z_{\phi_{\parallel}} = 2 + \zeta_{\Gamma_{\parallel}}^*, \quad z_m = 2 + \zeta_{\lambda}^* \quad (54)$$

to the dynamic ζ functions (see Ref. [3]). In Eq. (54) the short notation $\zeta_{\alpha_i}^* \equiv \zeta_{\alpha_i}(\{\alpha_j^*\})$ has been introduced. In the nonasymptotic background region effective dynamic exponents are defined as

$$z_{\perp}^{(\text{eff})}(l) = 2 + \zeta_{\Gamma_{\perp}}(\{\alpha_j(l)\}), \quad (55)$$

$$z_{\parallel}^{(\text{eff})}(l) = 2 + \zeta_{\Gamma_{\parallel}}(\{\alpha_j(l)\}), \quad (56)$$

$$z_m^{(\text{eff})}(l) = 2 + \zeta_{\lambda}(\{\alpha_j(l)\}), \quad (57)$$

where the flow of the parameters is inserted into the ζ functions instead of the FP values. The effective exponents depend on the flow parameter, or reduced temperature accordingly. Relation (53) makes sure that the effective exponents turn into the asymptotic exponents in the critical limit, that is,

$$\lim_{l \rightarrow 0} z_k^{(\text{eff})}(l) = z_{\phi_k} \quad \lim_{l \rightarrow 0} z_m^{(\text{eff})}(l) = z_m \quad (58)$$

with $k = \perp, \parallel$.

B. Time-scale ratios and mode-coupling parameters

It is convenient to introduce ratios of the kinetic coefficients or mode couplings, which may have finite FP values. The following ratios will be used in the subsequent sections:

(1) The time-scale ratios between the order parameters and the secondary density

$$w_{\perp} \equiv \frac{\Gamma_{\perp}}{\lambda}, \quad w_{\parallel} \equiv \frac{\Gamma_{\parallel}}{\lambda}. \quad (59)$$

From this we also define the ratio between kinetic coefficients of the two order parameters

$$v \equiv \frac{\Gamma_{\parallel}}{\Gamma_{\perp}} = \frac{w_{\parallel}}{w_{\perp}}, \quad (60)$$

which already previously has been used in the bicritical model A and model C. Note that in contrast to the two models mentioned, w_{\perp} and v are now complex quantities. The ratios in Eqs. (59) and (60) are of course not independent as shown by the equality in Eq. (60). The structure of the dynamic ζ functions presented subsequently further implies the introduction of the complex ratio

$$v_{\perp} \equiv \frac{\Gamma_{\perp}}{\Gamma_{\perp}^+} = \frac{w_{\perp}}{w_{\perp}^+} = \frac{v^+}{v}. \quad (61)$$

(2) The mode coupling parameter

$$F \equiv \frac{g}{\lambda} \quad (62)$$

does not necessarily have a finite FP value. Thus it may be more appropriate to use the ratio

$$f_{\perp} \equiv \frac{g}{\sqrt{\Gamma_{\perp}^+ \lambda}} = \frac{F}{\sqrt{w_{\perp}^+}} \quad (63)$$

in several cases, especially in the discussion of the flow equations and the fixed points.

The flow equations for the ratios defined above can be found from the ζ and β functions introduced in the previous subsection. From the definition of the parameters in Eqs. (59) and (63) and the renormalization (44) and (48) we obtain together with (49) the flow equations

$$l \frac{dw_{\perp}}{dl} = w_{\perp}(\zeta_{\Gamma_{\perp}} - \zeta_{\lambda}), \quad (64)$$

$$l \frac{dw_{\parallel}}{dl} = w_{\parallel}(\zeta_{\Gamma_{\parallel}} - \zeta_{\lambda}), \quad (65)$$

$$l \frac{df_{\perp}}{dl} = -\frac{f_{\perp}}{2} \left(\varepsilon + \zeta_{\lambda} - 2\zeta_m + \text{Re} \left[\frac{w_{\perp}}{w_{\perp}^+} \zeta_{\Gamma_{\perp}} \right] \right). \quad (66)$$

From (64) and (65) follows immediately the flow equation for the ratio

$$l \frac{dv}{dl} = v(\zeta_{\Gamma_{\parallel}} - \zeta_{\Gamma_{\perp}}), \quad (67)$$

which has been defined in Eq. (60).

The remaining task is to calculate the explicit expressions of the dynamic functions $\zeta_{\Gamma_{\perp}}$, $\zeta_{\Gamma_{\parallel}}$, and ζ_{λ} in two-loop order.

VI. DYNAMIC RG FUNCTIONS IN TWO-LOOP ORDER

The perturbation expansion of the dynamic vertex functions and the structures therein are outlined in detail in Appendix A. The resulting expressions for the dynamic renormalization factors in two-loop order are presented in Appendix B. With these expressions at hand we are in the position to obtain explicit two-loop expressions for the RG ζ functions.

A. Dynamic ζ functions of the OPs

Relations (45) and (46) between the Z factors imply the relations between the corresponding ζ functions:

$$\zeta_{\Gamma_{\perp}} = \zeta_{\Gamma_{\perp}}^{(d)} - \frac{1}{2}\zeta_{\tilde{\psi}^{\pm}} + \frac{1}{2}\zeta_{\psi}, \quad (68)$$

$$\zeta_{\Gamma_{\parallel}} = -\frac{1}{2}\zeta_{\tilde{\phi}_{\parallel}} + \frac{1}{2}\zeta_{\phi_{\parallel}}. \quad (69)$$

The static ζ functions $\zeta_{\psi} = \zeta_{\phi_{\perp}}$ have been presented in Eqs. (20) in paper I. Inserting (B1) and (B2) into (49) and (68) we obtain the dynamic ζ function for the kinetic coefficient of the perpendicular components as

$$\begin{aligned} \zeta_{\Gamma_{\perp}} = & \frac{D_{\perp}^2}{w_{\perp}(1+w_{\perp})} - \frac{2}{3} \frac{u_{\perp}D_{\perp}}{w_{\perp}(1+w_{\perp})} A_{\perp} \\ & - \frac{1}{2} \frac{D_{\perp}^2}{w_{\perp}^2(1+w_{\perp})^2} B_{\perp} \\ & - \frac{1}{2} \frac{\gamma_{\parallel}D_{\perp}}{1+w_{\perp}} \left(\frac{u_{\times}}{3} + \frac{1}{2} \frac{\gamma_{\parallel}D_{\perp}}{1+w_{\perp}} \right) X_{\perp} \\ & + \zeta_{\Gamma_{\perp}}^{(A)}(\{u\}, v_{\perp}, v), \end{aligned} \quad (70)$$

where we have introduced the coupling

$$D_{\perp} \equiv w_{\perp}\gamma_{\perp} - iF. \quad (71)$$

The functions A_{\perp} , B_{\perp} , and X_{\perp} are defined as

$$A_{\perp} \equiv w_{\perp}\gamma_{\perp}(1 - x_1L_1) + iFx_{\perp}x_1L_1 - D_{\perp}L_0, \quad (72)$$

$$\begin{aligned} B_{\perp} \equiv & w_{\perp}^2\gamma_{\perp}^2(1 - 2x_1L_1) + F^2(2x_{\perp}L_1 + L_R) \\ & + 2w_{\perp}\gamma_{\perp}iF(1 + 2x_{\perp}x_1L_1) - 2L_0D_{\perp}^2 \\ & - \frac{D_{\perp}^2}{1+w_{\perp}} \left[w_{\perp} + (1 + 2w_{\perp}) \ln \frac{(1+w_{\perp})^2}{1+2w_{\perp}} \right], \end{aligned} \quad (73)$$

$$X_{\perp} \equiv 1 + \ln \frac{2v}{1+v} - \left(1 + \frac{2}{v}\right) \ln \frac{2(1+v)}{2+v} \quad (74)$$

with

$$L_R \equiv [x_{+} + v_{\perp} + x_{+}^2(x_{+}^2 + 2v_{\perp}^2)] \frac{L_1}{x_{+}} - 3v_{\perp}. \quad (75)$$

We have used the following definitions in the above expressions:

$$x_{\pm} \equiv 1 \pm v_{\perp}, \quad x_1 \equiv 2 + v_{\perp}, \quad (76)$$

$$L_0 \equiv 2 \ln \frac{2}{1 + \frac{1}{v_{\perp}}}, \quad L_1 \equiv \ln \frac{(1 + \frac{1}{v_{\perp}})^2}{1 + 2\frac{1}{v_{\perp}}}. \quad (77)$$

$\zeta_{\Gamma_{\perp}}^{(A)}(\{u\}, v_{\perp}, v)$ is the ζ function of the kinetic coefficient of the perpendicular components in the bicritical model A, but now with a complex kinetic coefficient Γ_{\perp} . It reads in two-loop order

$$\zeta_{\Gamma_{\perp}}^{(A)}(\{u\}, v_{\perp}, v) = \frac{u_{\perp}^2}{9} \left(L_0 + x_1L_1 - \frac{1}{2} \right) + \frac{u_{\times}^2}{36} \left(L_{\perp}^{(\times)} - \frac{1}{2} \right) \quad (78)$$

with

$$L_{\perp}^{(\times)} \equiv \ln \frac{(1+v)^2}{v(2+v)} + \frac{2}{v} \ln \frac{2(1+v)}{2+v}. \quad (79)$$

The dynamic ζ function of the parallel component is obtained by inserting Eq. (21) of paper I and (B3) into (49) and (69). The result is

$$\begin{aligned} \zeta_{\Gamma_{\parallel}} = & \frac{w_{\parallel}\gamma_{\parallel}^2}{1+w_{\parallel}} - \frac{1}{2} \frac{w_{\parallel}\gamma_{\parallel}}{1+w_{\parallel}} \left\{ u_{\parallel}\gamma_{\parallel} \left(1 - 3 \ln \frac{4}{3}\right) + \frac{w_{\parallel}\gamma_{\parallel}^3}{1+w_{\parallel}} \left[\frac{1}{2} \left(1 - 9 \ln \frac{4}{3}\right) - \frac{w_{\parallel}}{1+w_{\parallel}} - \frac{1+2w_{\parallel}}{1+w_{\parallel}} \ln \frac{(1+w_{\parallel})^2}{1+2w_{\parallel}} \right] \right. \\ & \left. + \left(\frac{2}{3} u_{\times} + \frac{w_{\parallel}\gamma_{\parallel}}{1+w_{\parallel}} \gamma_{\perp} \right) \operatorname{Re} \left[\frac{T_1}{w'_{\perp}} \right] - \frac{\gamma_{\parallel}F}{2w'_{\perp}(1+w_{\parallel})} \operatorname{Im} \left[\frac{T_2}{w'_{\perp}} \right] \right\} + \zeta_{\Gamma_{\parallel}}^{(A)}(\{u\}, v_{\perp}, v). \end{aligned} \quad (80)$$

The functions T_1 and T_2 are defined as

$$\begin{aligned} T_1 \equiv & D_{\perp} \left\{ 1 + \ln \frac{1 + \frac{1}{v_{\perp}}}{1+v} \right. \\ & \left. - \left[v + \frac{1}{v_{\perp}}(1+v) \right] \ln \frac{(1+v)(1 + \frac{1}{v_{\perp}})}{v + \frac{1}{v_{\perp}}(1+v)} \right\}, \end{aligned} \quad (81)$$

$$\begin{aligned} T_2 \equiv & w_{\perp}^{\dagger} D_{\perp} \left\{ (1+v_{\perp})v - \ln \frac{1 + \frac{1}{v_{\perp}}}{1+v} \right. \\ & \left. - \left[v + \frac{1}{v_{\perp}}(1+v) \right] [v + v_{\perp}(1+v)] \ln \frac{(1+v)(1 + \frac{1}{v_{\perp}})}{v + \frac{1}{v_{\perp}}(1+v)} \right\}, \end{aligned} \quad (82)$$

$\zeta_{\Gamma_{\parallel}}^{(A)}(\{u\}, v_{\perp}, v)$ is the ζ function of the kinetic coefficient of the parallel component in the bicritical model A. With a complex Γ_{\perp} it reads

$$\zeta_{\Gamma_{\parallel}}^{(A)}(\{u\}, v_{\perp}, v) = \frac{u_{\parallel}^2}{4} \left(\ln \frac{4}{3} - \frac{1}{6} \right) + \frac{u_{\times}^2}{18} \left(L_{\parallel}^{(\times)} - \frac{1}{2} \right) \quad (83)$$

with

$$\begin{aligned} L_{\parallel}^{(\times)} \equiv & \ln \frac{(1+v)(\frac{1}{v_{\perp}} + v)}{v + \frac{1}{v_{\perp}}(1+v)} + vv_{\perp} \ln \frac{(1 + \frac{1}{v_{\perp}})(\frac{1}{v_{\perp}} + v)}{v + \frac{1}{v_{\perp}}(1+v)} \\ & + v \ln \frac{(1 + \frac{1}{v_{\perp}})(1+v)}{v + \frac{1}{v_{\perp}}(1+v)}. \end{aligned} \quad (84)$$

B. Dynamic ζ functions of the secondary density

With relation (47) we can separate the static contributions to the ζ function ζ_λ . Thus we have

$$\zeta_\lambda = 2\zeta_m + \zeta_\lambda^{(d)}. \quad (85)$$

By separating the static from the dynamic parts in the ζ functions one can take advantage of the general structures appearing in the purely dynamic ζ function $\zeta_\lambda^{(d)}$ as well as in the static ζ function ζ_m . Inserting $n_\perp = 2$ and $n_\parallel = 1$ into relation (40) in paper III ζ_m can be written as

$$\zeta_m = \frac{1}{2}\gamma_\perp^2 + \frac{1}{4}\gamma_\parallel^2, \quad (86)$$

which is valid up to two-loop order. From the diagrammatic structure of the dynamic perturbation theory follows

$$\zeta_\lambda^{(d)} = -\frac{f_\perp^2}{2}(1 + \mathcal{Q}). \quad (87)$$

The real function \mathcal{Q} contains all higher-order contributions beginning with two-loop order. Setting $\mathcal{Q} = 0$ in Eq. (87) reproduces the one-loop expressions of this function. The function \mathcal{Q} in the dynamic ζ function of the secondary density (87) has the structure

$$\mathcal{Q} = \frac{1}{2} \text{Re}[X_2] \quad (88)$$

from which immediately follows that it is a real quantity. X_2 reads

$$X_2 = \frac{D_\perp}{w'_\perp(1+w_\perp)} \left[D_\perp \left(\frac{1}{2} + \ln \frac{1+w_\perp}{1+w_\perp^+} \right) + D_\perp^+(1+w_\perp) - (W_\perp^{(m)}\gamma_\perp + w_\perp iF)W_\perp^{(m)}L_\perp^{(m)} \right], \quad (89)$$

where we have introduced the definitions

$$L_\perp^{(m)} = \ln \left(1 + \frac{1}{W_\perp^{(m)}} \right), \quad (90)$$

$$W_\perp^{(m)} = w_\perp + w_\perp^+ + w_\perp w_\perp^+. \quad (91)$$

Note that X_2 coincides with the corresponding function in model F in Refs. [3,22].

VII. CRITICAL BEHAVIOR IN ONE-LOOP ORDER

Although the one-loop critical behavior of the considered system has already been discussed in Ref. [6] we want to summarize the results in order to compare it with the considerably differing results of the two-loop calculation. In one-loop order the ζ functions (70), (80), and (87) reduce to

$$\zeta_{\Gamma_\perp} = \frac{D_\perp^2}{w_\perp(1+w_\perp)}, \quad \zeta_{\Gamma_\parallel} = \frac{w_\parallel\gamma_\parallel^2}{1+w_\parallel}, \quad \zeta_\lambda^{(d)} = -\frac{f_\perp^2}{2}. \quad (92)$$

Inserting (92) into the right-hand sides of (64)–(66) leads to a set of equations in which the zeros determine the dynamical FPs. The only stable FP is found for $w_\parallel^* = 0$ and w_\perp^* , w_\perp^{**} , and f_\perp^* finite. The corresponding values are presented in Table II. As a consequence we have $v^* = 0$. We note that the static FP values of the two-loop calculation in papers I and III have been used. We were interested in the nonasymptotic properties described by flow equations, and since no real FP in statics is reached in two-loop order, we had to resume the static β functions in order to get real FP values [2]. To each type of static FP (biconical or Heisenberg) two equivalent static fixed points exist, differing in the signs of γ_\perp and γ_\parallel [11]. Accordingly four equivalent dynamic fixed points exist with different signs in w_\perp^* and f_\perp^* . They correspond to the directions of the external fields of the parallel and perpendicular OP.

The finite value of w_\perp^* implies the relations

$$\zeta_{\Gamma_\perp}^* = \zeta_\lambda^*, \quad \zeta_{\Gamma_\perp}^{**} = 0, \quad \varepsilon + \zeta_{\Gamma_\perp}^* + \zeta_\lambda^* - 2\zeta_m^* = 0, \quad (93)$$

which follow from (64) and (66). The vanishing w_\parallel^* leads to $\zeta_{\Gamma_\parallel}^* = 0$ as can immediately be seen from (92). Using the first relation in Eq. (93) and the third one, we obtain

$$\zeta_{\Gamma_\perp}^{**} = \zeta_\lambda^* = \frac{1}{2}(2\zeta_m^* - \varepsilon). \quad (94)$$

Inserting the FP value of the static ζ function ζ_m^* [see relation (105) in paper III]

$$\zeta_m^* = \frac{\phi}{v} - \frac{d}{2} \quad (95)$$

into the above equation, one has

$$\zeta_{\Gamma_\perp}^{**} = \zeta_\lambda^* = \frac{\phi}{v} - 2. \quad (96)$$

The dynamic critical exponents (54) in one-loop order are therefore completely expressed in terms of the static

TABLE II. FP values of couplings and time-scale ratios for $n_\parallel = 1$, $n_\perp = 2$ at $d = 3$. \mathcal{B} indicates the biconical, \mathcal{H} the Heisenberg FP. There are always two equivalent static FPs depending on the signs of the couplings γ . The FP values of the static couplings $\{u\}$ and $\{\gamma\}$ are taken from the resummed two-loop results [2], whereas w_\perp^* and f_\perp^* are calculated from the one-loop β functions. $w_\parallel^* = v^* = 0$ is valid in all cases. Corresponding to the two equivalent cases in statics and the sign of w_\perp^{**} there are equivalent dynamic FPs with corresponding signs of the FP value of the mode coupling f_\perp^* .

FP	u_\parallel^*	u_\perp^*	u_x^*	γ_\parallel^*	γ_\perp^*	w_\perp^*	w_\perp^{**}	f_\perp^*
\mathcal{B}	1.28745	1.12769	0.30129	0.54201	-0.17806	1.55489	∓ 0.41958	± 1.08563
\mathcal{B}	1.28745	1.12769	0.30129	-0.54201	0.17806	1.55489	± 0.41958	± 1.08563
\mathcal{H}	1.00156	1.00156	1.00156	0.85179	-0.42590	1.58136	∓ 1.38256	± 1.24264
\mathcal{H}	1.00156	1.00156	1.00156	-0.85179	0.42590	1.58136	± 1.38256	± 1.24264

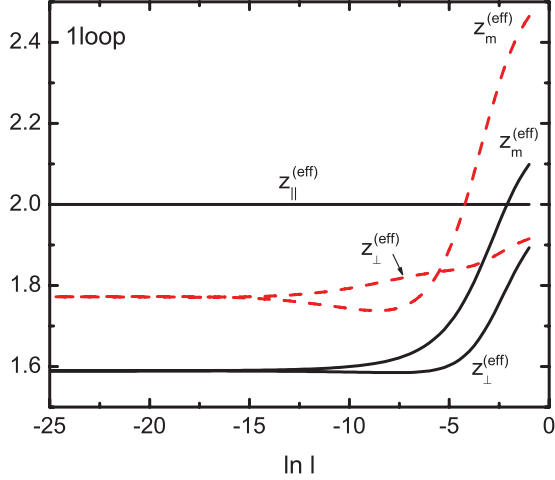


FIG. 1. (Color online) Effective dynamic exponents at $d = 3$ calculated in one-loop order using the one-loop expression for the flow equations (64) and (66). The effective exponents are calculated at the biconical FP (full lines) and at the Heisenberg FP (dashed line). $z_{\parallel}^{(\text{eff})}$ is valid for both FPs.

exponents:

$$z_{\phi_{\perp}} = z_m = \frac{\phi}{\nu}, \quad z_{\phi_{\parallel}} = 2. \quad (97)$$

These static exponents might also be taken from static experiments. All our numerical calculations are performed in $d = 3$ ($\epsilon = 1$). The numerical values of the static exponents ϕ and ν have been calculated in two-loop order in paper I and are given there in Table III ($\nu = \nu_+$ therein) in two-loop

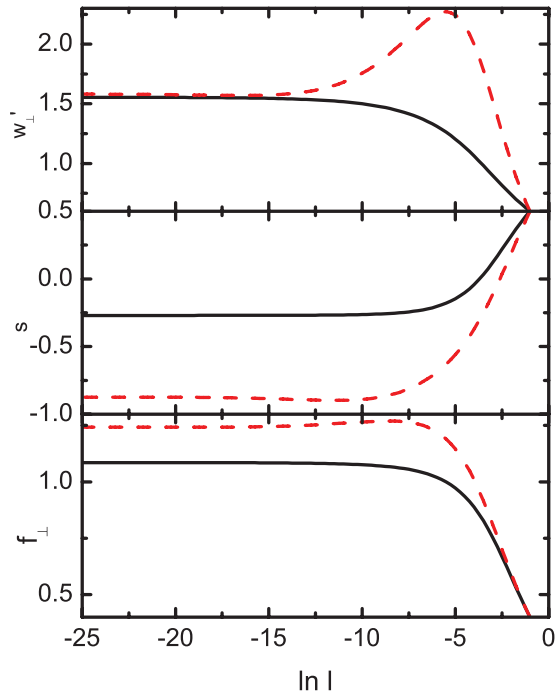


FIG. 2. (Color online) Flow of the parameters w'_{\perp} , $s = w''_{\perp}/w'_{\perp}$, and f_{\perp} in one-loop order at $d = 3$. The calculation has been performed for the biconical (solid lines) and the Heisenberg (dashed lines) FP.

order resummed. In one-loop order the two OPs have different dynamic critical exponents. Scaling is fulfilled only between the perpendicular OP and the secondary density. The parallel OP behaves like the van Hove model. This is demonstrated in Fig. 1, where the effective exponents defined in (55)–(57) have been calculated by using the dynamic flow equations in one-loop order. At a flow parameter about $l \sim e^{-15}$ for both, the biconical FP (solid lines) and the Heisenberg FP (dashed lines), the asymptotic values $z_{\phi_{\perp}}$, z_m of the effective dynamic exponents $z_{\perp}^{(\text{eff})}$ and $z_m^{(\text{eff})}$ are reached. The classical value $z_{\phi_{\parallel}} = 2$, valid for both static fixed points, also is indicated by a straight line. The corresponding flow is presented in Fig. 2, which proves that the dynamic exponents in Fig. 1 have reached their asymptotic behavior because the dynamic parameters are at their FP values at $\ln l = -25$.

VIII. LIMITING BEHAVIOR OF THE DYNAMICAL ζ FUNCTIONS IN TWO-LOOP ORDER

The appearance of $\ln v$ terms in the two-loop contribution to the $\zeta_{\Gamma_{\perp}}$ function, Eq. (70), changes the discussion of the fixed points considerably compared to the one-loop case. In order to determine the dynamical fixed points of the current model in two-loop order it is necessary to know something about the limiting behavior of the ζ functions. For this reason we will present the ζ functions in cases where one or several dynamical parameters go to zero or infinity under definite conditions. This is necessary because some ζ functions exhibit singular behavior under these conditions, which influences the discussion of possible fixed points. It is anticipated that the critical exponents defined by the values of the ζ functions at the FP are finite and real.

The auxiliary functions X_{\perp} , $L_{\perp}^{(\times)}$, T_1 , T_2 , and $L_{\parallel}^{(\times)}$, which appear in the ζ functions (70) and (80), behave singularly in several limits of the parameters. Thus several FP values of the different parameters can be excluded due to diverging ζ functions. For a summary of the subsequent analysis of the ζ function on the time-scale ratios see Table III.

(1) First, we will consider the two functions X_{\perp} and $L_{\perp}^{(\times)}$ in Eqs. (74) and (79), which appear in $\zeta_{\Gamma_{\perp}}$ and depend on v only. These two functions remain regular if v grows to infinity. In this case one simply has $X_{\perp}(v \rightarrow \infty) = 1$ and $L_{\perp}^{(\times)}(v \rightarrow \infty) = 0$. But for vanishing v both functions evolve a term proportional to $\ln v$. One gets

$$X_{\perp}(v \rightarrow 0) \sim \ln(2v), \quad L_{\perp}^{(\times)}(v \rightarrow 0) \sim -\ln(2v). \quad (98)$$

TABLE III. Limiting behavior of the dynamic ζ functions.

Limit	$\zeta_{\Gamma_{\perp}}$	$\zeta_{\Gamma_{\parallel}}$	ζ_{λ}
$v \rightarrow 0$	$\sim \ln v$	Regular	Unaffected
$v \rightarrow \infty$	Regular	$\sim \ln v$	Unaffected
$w_{\perp} \rightarrow \infty$	$\sim \ln w_{\perp}$	Regular	$\sim w_{\perp}^2$
$w_{\parallel} \rightarrow \infty$	Regular	$\sim \ln w_{\parallel}$	Unaffected
$w_{\perp} \rightarrow 0$	Regular	$\sim \ln v$	Regular
$w_{\parallel} \rightarrow 0$	$\sim \ln v$	Regular	Unaffected

Thus divergent $\ln v$ terms appear in $\zeta_{\Gamma_{\perp}}(v \rightarrow 0)$ independent from the individual behavior of w_{\perp} and w_{\parallel} because only the ratio v enters the function.

(2) The dynamic ζ function (80) of the parallel component contains the three functions T_1 , T_2 , and $L_{\parallel}^{(\times)}$ defined in Eqs. (81), (82), and (84), which contain the ratio v . These functions, and therefore also $\zeta_{\Gamma_{\parallel}}$, remain nondivergent for vanishing v . One obtains

$$\begin{aligned} T_1(v \rightarrow 0) &= D_{\perp} \left[1 + \ln \left(1 + \frac{1}{v_{\perp}} \right) - \frac{1}{v_{\perp}} \ln(1 + v_{\perp}) \right], \\ T_2(v \rightarrow 0) &= -w_{\perp}^* D_{\perp} \left[\ln \left(1 + \frac{1}{v_{\perp}} \right) + \ln(1 + v_{\perp}) \right], \\ L_{\parallel}^{(\times)}(v \rightarrow 0) &= 0. \end{aligned} \quad (99)$$

But they diverge when v is growing to infinity:

$$\begin{aligned} T_1(v \rightarrow \infty) &\sim D_{\perp} \ln \frac{(1 + \frac{1}{v_{\perp}})}{v}, \\ T_2(v \rightarrow \infty) &\sim -w_{\perp}^* D_{\perp} \ln \frac{(1 + \frac{1}{v_{\perp}})}{v}, \\ L_{\parallel}^{(\times)}(v \rightarrow \infty) &\sim \ln \frac{v}{(1 + \frac{1}{v_{\perp}})}. \end{aligned} \quad (100)$$

In contrast to the case (1) the function $\zeta_{\Gamma_{\parallel}}$ in the parallel subspace evolves logarithmic terms $\ln v$ in the limit $v \rightarrow \infty$ and stays finite in the limit $v \rightarrow 0$. The above discussion is also independent of the individual behavior of w_{\perp} and w_{\parallel} because only the ratio v_{\perp} stays always finite, and the three functions T_1 , T_2 and $L_{\parallel}^{(\times)}$ remain finite even for diverging time-scale ratios if their prefactors are taken into account.

(3) Additional logarithmic singularities may arise in the dynamic ζ functions if the time-scale ratios w_{\perp} and w_{\parallel} grow individually to infinity independent of the behavior of v . A closer examination of (70) reveals that in the limit $w_{\perp} \rightarrow \infty$ the ζ function is proportional to

$$\zeta_{\Gamma_{\perp}}(w_{\perp} \rightarrow \infty) \sim \frac{1}{2} \gamma_{\perp}^4 \ln \frac{w_{\perp}}{2} \quad (101)$$

independent of the behavior of v . Quite analogously the same happens in Eq. (80) when w_{\parallel} grows to infinity. One obtains

$$\zeta_{\Gamma_{\parallel}}(w_{\parallel} \rightarrow \infty) \sim \frac{1}{2} \gamma_{\parallel}^4 \ln \frac{w_{\parallel}}{2}. \quad (102)$$

Supposing a finite (different from zero or infinity) FP value f_{\perp}^* for the mode coupling parameter we may conclude the following concerning the allowed FP values of the remaining parameters:

(a) From (1) and (2) follows that v^* has to be also different from zero or infinity, otherwise $\ln v$ contributions would lead to divergent ζ functions.

(b) From (3) follows that the finite v^* can be realized only either by w_{\parallel} and w_{\perp} both finite, or w_{\parallel} and w_{\perp} both going to zero in the same way. The possibility that both time-scale ratios are going to infinity in the same way is excluded because of the $\ln w_{\parallel}$ and $\ln w_{\perp}$ terms appearing in this case.

IX. GENERAL ASYMPTOTIC RELATIONS

The FP values $\{\alpha_j^*\}$ of the model parameters are found from the zeros of the β functions in Eqs. (64)–(66). From the right-hand side of the equations one obtains

$$w_{\perp}^*(\zeta_{\Gamma_{\perp}}^* - \zeta_{\lambda}^*) = 0, \quad (103)$$

$$w_{\parallel}^*(\zeta_{\Gamma_{\parallel}}^* - \zeta_{\lambda}^*) = 0, \quad (104)$$

$$f_{\perp}^* \left(\varepsilon + \zeta_{\lambda}^* - 2\zeta_m^* + \operatorname{Re} \left[\frac{w_{\perp}^*}{w_{\perp}^*} \zeta_{\Gamma_{\perp}}^* \right] \right) = 0. \quad (105)$$

A FP that fulfills Eqs. (103)–(105) has to be also a solution of

$$v^*(\zeta_{\Gamma_{\parallel}}^* - \zeta_{\Gamma_{\perp}}^*) = 0, \quad (106)$$

which follows from (67). The ζ function $\zeta_{\Gamma_{\perp}}$ for the perpendicular component of the OP relaxation is a complex function. Separating real and imaginary part leads to

$$\zeta_{\Gamma_{\perp}} = \zeta'_{\Gamma_{\perp}} + i\zeta''_{\Gamma_{\perp}}. \quad (107)$$

As a consequence also the equations (103) for w_{\perp} and (106) for v are complex expressions. The ζ function for Γ'_{\perp} is

$$\zeta_{\Gamma'_{\perp}} = \zeta'_{\Gamma_{\perp}} - \frac{w''_{\perp}}{w'_{\perp}} \zeta''_{\Gamma_{\perp}}. \quad (108)$$

We anticipate that in a real physical system definite dynamical exponents exist, and therefore the dynamic ζ functions have to be finite at the stable FP. As already mentioned in Sec. VIII, the ζ functions contain $\ln v$ terms requiring a finite FP value v^* in order to obtain finite dynamical exponents. Separating (106) into real and imaginary part, one has

$$v^{*\prime}(\zeta'_{\Gamma_{\perp}} - \zeta'_{\Gamma_{\parallel}}) - v^{*\prime\prime} \zeta''_{\Gamma_{\perp}} = 0, \quad (109)$$

$$v^{*\prime} \zeta''_{\Gamma_{\perp}} + v^{*\prime\prime}(\zeta'_{\Gamma_{\perp}} - \zeta'_{\Gamma_{\parallel}}) = 0. \quad (110)$$

From these two equations the FP relations

$$\zeta_{\Gamma_{\perp}}^{*\prime} = \zeta_{\Gamma_{\parallel}}^{*\prime}, \quad \zeta_{\Gamma_{\perp}}^{*\prime\prime} = 0 \quad (111)$$

immediately follow. The second equation in Eq. (111) implies that the dynamical exponent $z_{\phi_{\perp}}$ in Eq. (54) can be written as

$$z_{\phi_{\perp}} = 2 + \zeta_{\Gamma_{\perp}}^{*\prime}. \quad (112)$$

From the first relation in Eq. (111) follows

$$z_{\phi_{\perp}} = z_{\phi_{\parallel}}. \quad (113)$$

This means that in the case of a finite FP value v^* scaling between the OPs is valid. In order to obtain a critical behavior different from model C, the FP value f_{\perp}^* of the mode coupling parameter also has to be finite and different from zero. Then from Eq. (105) follows

$$\varepsilon + \zeta_{\Gamma_{\perp}}^{*\prime} + \zeta_{\lambda}^* - 2\zeta_m^* = 0, \quad (114)$$

where the second relation of (111) already has been used. Inserting (85) and (95) into (114) one obtains the relation

$$z_{\phi_{\perp}} + z_m = 2 \frac{\phi}{v} \quad (115)$$

between the exponents. In summary, the condition that both v^* and f_{\perp}^* have to be finite leads to the two relations (113) and

(115) between the exponents. Further relations are dependent whether the FP values of the time-scale ratios w_{\perp} and w_{\parallel} are finite or zero and lead to the following cases.

1. Dynamical strong scaling FP

In the case that w_{\perp} and w_{\parallel} are finite at the FP, from (103) and (104) the relation

$$\zeta_{\Gamma_{\perp}}^{\prime*} = \zeta_{\Gamma_{\parallel}}^{\prime*} = \zeta_{\lambda}^{\prime*} \quad (116)$$

is obtained, where (111) already has been used. From (54) it follows immediately that the dynamical exponents have to fulfill the relations

$$z_{\phi_{\perp}} = z_{\phi_{\parallel}} = z_m \equiv z. \quad (117)$$

Thus in the case of strong scaling one dynamical exponent z exists only. The exact value of this exponent can be found by inserting (117) into (115). One obtains

$$z = \frac{\phi}{\nu}. \quad (118)$$

2. Dynamical weak scaling FP

In the case that w_{\perp} and w_{\parallel} are zero with ν finite at the FP, Eqs. (103) and (104) are trivially fulfilled, and no additional relation between the ζ functions and dynamical exponents, respectively, arises. As a consequence two dynamical exponents exist. The first one,

$$z_{\phi_{\parallel}} = z_{\phi_{\perp}} = z_{\text{OP}} \quad (119)$$

for the OPs, follows from relation (113). The second one,

$$z_m = 2\frac{\phi}{\nu} - z_{\text{OP}} \quad (120)$$

for the secondary density, is obtained from (115).

A closer examination of the β functions (103)–(105), also with numerical methods in $d = 3$, reveals that no FP solution can be found where both w_{\perp} and w_{\parallel} are finite. Thus the only solution in $d = 3$ that remains is $w_{\perp}^{\prime*} = w_{\parallel}^{\prime*} = w_{\parallel}^* = 0$ with ν^*

and ν_{\perp}^* finite. This result, of course, depends also on the specific numerical values [23] of the static FPs (given in Table II) used in the dynamical equations. The stable FP lies then in the subspace where the time-scale ratios w_{\parallel} and w_{\perp} approach zero in such a way that their ratios ν and ν_{\perp} remain finite and in general complex quantities. In order to obtain the finite FP values for ν and ν_{\perp} the two-loop ζ functions may be reduced by setting w_{\perp} and w_{\parallel} equal to zero and keeping their ratios finite. This will be performed in the following section.

X. CRITICAL BEHAVIOR IN THE ASYMPTOTIC SUBSPACE

Since the asymmetric couplings γ_{α} always appear together with the time-scale ratios w_{α} , all terms proportional to these couplings drop out in the asymptotic limit where $w_{\alpha} \rightarrow 0$. It is convenient to introduce the real ratios

$$s \equiv \frac{w_{\perp}''}{w_{\perp}'} = \frac{\Gamma_{\perp}''}{\Gamma_{\perp}'}, \quad q \equiv \frac{w_{\parallel}}{w_{\perp}'} = \frac{\Gamma_{\parallel}}{\Gamma_{\perp}'}. \quad (121)$$

Thus only s , q , and f_{\perp} remain as independent dynamical variables.

The ratio s determines the behavior of the imaginary part of w_{\perp} with respect to the real part, while the ratio q indicates the behavior of w_{\parallel} with respect to the real part of w_{\perp} . The complex parameters ν_{\perp} and ν , introduced in Eqs. (61) and (60), are expressed by s and q as

$$\nu_{\perp} = \frac{1 + is}{1 - is}, \quad \nu = \frac{q}{1 + is} \quad (122)$$

in the following expressions.

A. ζ functions

We discuss the behavior of the ζ functions in the limit $w_{\perp} \rightarrow 0$ and $w_{\parallel} \rightarrow 0$ for s and q constant.

1. Case $s \neq 0$

For $w_{\perp} = 0$ and $w_{\parallel} = 0$ the ζ function (70) reduces to

$$\zeta_{\Gamma_{\perp}}^{(\text{as})}(\{u\}, s, q, f_{\perp}) = -\frac{f_{\perp}^2}{1 + is} \left\{ 1 + \frac{2}{3} u_{\perp} [L_0(s) + x_{-}(s)x_1(s)L_1(s)] - \frac{1}{2} \frac{f_{\perp}^2}{1 + is} [2x_{-}(s)L_1(s) - 2L_0(s) + L_R(s)] \right\} + \zeta_{\Gamma_{\perp}}^{(A)}(\{u\}, s, q). \quad (123)$$

The functions $x_{-}(s)$, $x_1(s)$, $L_0(s)$, $L_1(s)$, and $L_R(s)$ are the same as in Eqs. (75)–(77) with ν_{\perp} replaced by (122). The same is true for $\zeta_{\Gamma_{\perp}}^{(A)}(\{u\}, s, q)$, which has been defined in Eq. (78), and where also (122) has been used to replace ν_{\perp} and ν .

Performing the limit in the dynamical ζ function (80) it reduces to

$$\zeta_{\Gamma_{\parallel}}^{(\text{as})}(\{u\}, s, q) = \zeta_{\Gamma_{\parallel}}^{(A)}(\{u\}, s, q) \quad (124)$$

where $\zeta_{\Gamma_{\parallel}}^{(A)}(\{u\}, s, q)$ is the model A function (83) with relation (122) inserted into (84).

Finally the function X_2 in Eq. (89) simplifies for vanishing time-scale ratios to

$$X_2^{(\text{as})}(f_{\perp}) = \frac{f_{\perp}^2}{2}. \quad (125)$$

Inserting this expression into (88) and (87), the dynamical ζ function (85) reads

$$\zeta_{\lambda}^{(\text{as})}(\{\gamma\}, f_{\perp}) = \gamma_{\perp}^2 + \frac{1}{2} \gamma_{\parallel}^2 - \frac{f_{\perp}^2}{2} \left(1 + \frac{f_{\perp}^2}{4} \right). \quad (126)$$

The value of v_{\perp} at the FP depends on how w'_{\perp} goes to zero in the critical limit $l \rightarrow 0$ compared to w''_{\perp} . There are three possible scenarios:

(1) w''_{\perp} goes to zero faster than w'_{\perp} so that $s \rightarrow 0$. Then v_{\perp} is turning to the real value 1.

(2) w'_{\perp} and w''_{\perp} behave in the same way so that the ratio $s = s_0$ is constant. v_{\perp} is in this case a complex constant

$$v_{\perp} = \frac{1 + is_0}{1 - is_0}. \quad (127)$$

(3) w'_{\perp} goes to zero faster than w''_{\perp} so that $s \rightarrow \infty$. Then v_{\perp} is turning to the real value -1 .

The third of the three scenarios above can be excluded from the discussion because some of the ζ functions do not stay finite for $v_{\perp} = -1$. Finite ζ functions at the FP and therefore well-defined critical exponents are obtained only in the first two scenarios.

The ζ function for scenario (2) is already given in Eqs. (123)–(126) when (127) is inserted.

2. Case $s = 0$

For $v_{\perp} = 1$ ($s = 0$) the ζ functions (123) and (124) simplify to

$$\zeta_{\Gamma_{\perp}}^{(\text{as}0)}(\{u\}, q, f_{\perp}) = -f_{\perp}^2 \left[1 - \frac{f_{\perp}^2}{2} \left(\frac{27}{2} \ln \frac{4}{3} - 3 \right) \right] + \zeta_{\Gamma_{\perp}}^{(A0)}(\{u\}, q), \quad (128)$$

$$\zeta_{\Gamma_{\parallel}}^{(\text{as}0)}(\{u\}, q) = \zeta_{\Gamma_{\parallel}}^{(A0)}(\{u\}, q). \quad (129)$$

The model A functions (78) and (83) are now

$$\zeta_{\Gamma_{\perp}}^{(A0)}(\{u\}, q) = \frac{u_{\perp}^2}{9} \left(3 \ln \frac{4}{3} - \frac{1}{2} \right) + \frac{u_{\times}^2}{36} \left[L_{\perp}^{(\times)}(q) - \frac{1}{2} \right] \quad (130)$$

and

$$\zeta_{\Gamma_{\parallel}}^{(A0)}(\{u\}, q) = \frac{u_{\parallel}^2}{4} \left(\ln \frac{4}{3} - \frac{1}{6} \right) + \frac{u_{\times}^2}{18} \left[L_{\parallel}^{(\times)}(q) - \frac{1}{2} \right], \quad (131)$$

where in $L_i^{(\times)}(q)$, introduced in Eqs. (79) and (84), the relations (122) with $s = 0$ have been inserted.

B. Fixed points in the asymptotic subspace

Inserting the ζ functions of the previous subsection into (103)–(105) one obtains the FP values in the asymptotic subspace for s^* finite, or $s^* = 0$. The results are presented in Table IV for the biconical (\mathcal{B}) and the Heisenberg (\mathcal{H}) FP. It turns out that especially at the biconical FP the values of the ratio q are extremely small, but definitely not zero. Thus the asymptotic critical behavior in two-loop order changes considerably compared to one-loop (see Sec. VII). Weak scaling as discussed in Sec. IX is valid. The two-order parameters scale with the same dynamic exponent z_{OP} from relation (119), while the secondary density scales with a different dynamic exponent z_m given in Eq. (120). The numerical values of these two dynamic exponents are also given in Table IV in two-loop order. Note that the values of the

TABLE IV. FP values of the mode coupling f_{\perp} and the ratios $q = w_{\parallel}/w'_{\perp}$ and $s = w''_{\perp}/w'_{\perp}$ in the subspace $w_{\parallel} = 0$, $w_{\perp} = 0$ and finite $v = q/(1 + is)$ for different cases of the biconical \mathcal{B} and Heisenberg \mathcal{H} FP in $d = 3$. For comparison results for model C and model F FPs are shown at $n = 1$ and $n = 2$, correspondingly.

	f_{\perp}^*	q^*	s^*	z_{OP}	z_m
C [9]	–	–	0	2.18	2.18
F [10]	0.83	–	0	~ 1.5	~ 1.5
\mathcal{B}	1.232	1.167×10^{-86}	0	2.048	1.131
\mathcal{H}	1.211	3.324×10^{-8}	0	2.003	1.542
\mathcal{B}	1.232	2.51×10^{-782}	0.705	2.048	1.131
\mathcal{H}	1.211	3.16×10^{-66}	0.698	2.003	1.542

dynamical exponents to the accuracy shown are independent whether the FP value of s is zero or not.

The comparison with the dynamical critical exponents in the cases when the OPs decouple statically and dynamically into model C and model F shows the changes in the multicritical case where the exponents are changed but each component reflects the decoupled values accordingly.

C. Effective exponents in the asymptotic subspace

The flow of the parameters q , s and f_{\perp} can be found by solving the equations

$$l \frac{dq}{dl} = q (\zeta_{\Gamma_{\parallel}}^{(\text{as})} - \text{Re}[\zeta_{\Gamma_{\perp}}^{(\text{as})}] + s \text{Im}[\zeta_{\Gamma_{\perp}}^{(\text{as})}]), \quad (132)$$

$$l \frac{ds}{dl} = (1 + s^2) \text{Im}[\zeta_{\Gamma_{\perp}}^{(\text{as})}], \quad (133)$$

$$l \frac{df_{\perp}}{dl} = -\frac{f_{\perp}}{2} (\varepsilon + \zeta_{\lambda}^{(\text{as})} - 2\zeta_m + \text{Re}[\zeta_{\Gamma_{\perp}}^{(\text{as})}] - \text{Im}[\zeta_{\Gamma_{\perp}}^{(\text{as})}]). \quad (134)$$

The ζ functions in the above flow equations are the reduced expressions (123), (124), and (126), which are functions of q, s, f_{\perp} . We consider the case $s \neq 0$ since the FP $s^* = 0$ is reached only starting with $s = 0$. From the solution of Eqs. (133) and (134) the flow $q(l), s(l), f_{\perp}(l)$ is obtained, which is used to calculate asymptotic effective dynamic exponents

$$z_{\perp}^{(\text{as})}(l) = 2 + \text{Re}[\zeta_{\Gamma_{\perp}}^{(\text{as})}(q(l), s(l), f_{\perp}(l))] - s(l) \text{Im}[\zeta_{\Gamma_{\perp}}^{(\text{as})}(q(l), s(l), f_{\perp}(l))], \quad (135)$$

$$z_{\parallel}^{(\text{as})}(l) = 2 + \zeta_{\Gamma_{\parallel}}^{(\text{as})}(q(l), s(l)), \quad (136)$$

$$z_m^{(\text{as})}(l) = 2 + \zeta_{\lambda}^{(\text{as})}(q(l), s(l), f_{\perp}(l)). \quad (137)$$

They can be calculated for different static fixed points, i.e., biconical or Heisenberg FP, as presented in Fig. 3. The values of u_{\perp}^* , u_{\parallel}^* , u_{\times}^* , as well as γ_{\perp}^* , γ_{\parallel}^* , used in the current calculations can be found in Table II. At both fixed points weak scaling, as discussed in Sec. IX, is fulfilled. The difference to the one-loop result is now that the dynamic exponents $z_{\perp}^{(\text{as})}$ and $z_{\parallel}^{(\text{as})}$ of the OPs are equal in the asymptotic region, while $z_m^{(\text{as})}$ stays different. Moreover the transient exponents in two-loop order are very small compared to one loop. There the effective exponents reach their asymptotic values about $l \sim e^{-15}$ as can be seen from Fig. 1. In two-loop order the asymptotic region

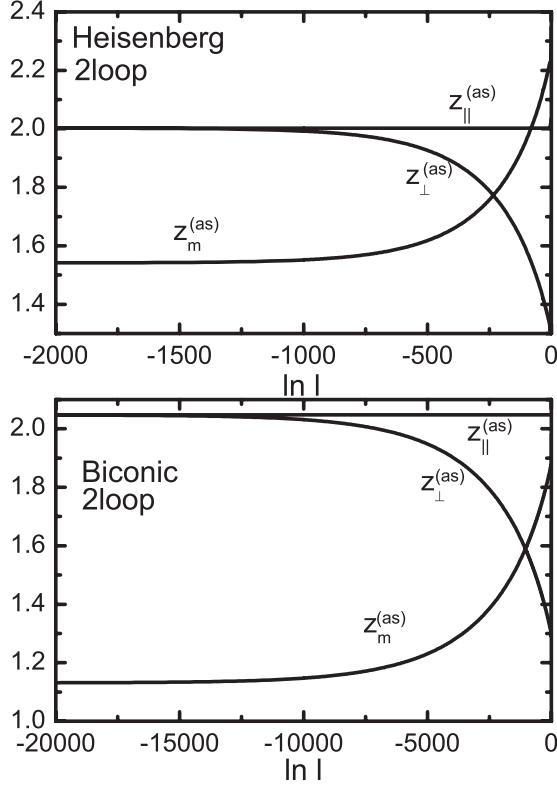


FIG. 3. Effective dynamic exponents in the subspace $w_{\parallel} = w_{\perp} = 0$ with q and s finite in $d = 3$. The static values are taken for the Heisenberg FP and for the biconical FP. The nonasymptotic region is extended by a factor 10 at the biconical FP. For the static FP values, see Table II; for the dynamic FP values, see Table IV.

is of magnitudes smaller. From Fig. 3 one can see that at the Heisenberg FP the flow parameter has to be of the order $l \sim e^{-1500}$ to obtain the asymptotic values of the dynamic exponents. At the biconical FP l has to be even of the order $l \sim e^{-15000}$ (note that there is a factor 10 between the x scales in Fig. 3) to reach asymptotic values. However, as will be seen in the next section the subspace will not be reached by the flow in the complete parameter space for reasonable values of l .

XI. GENERAL FLOW AND PSEUDO-ASYMPTOTICS

Although in general the dynamic flow equations have to be solved in the full parameter space, the results for the effective exponents presented in the previous subsection are obtained from the flow equations, which already have been reduced to the subspace $w_{\perp} = w_{\parallel} = 0$. The reason to do this is that the flow and the ζ functions in the full parameter space show peculiar behavior.

In the nonasymptotic region the flow is generated by the system of equations for four parameters, which are w'_{\perp} , s , w_{\parallel} , and f_{\perp} obtained from Eqs. (64)–(66) and (121). The static parameters are taken at their FP values given in Table II. Due to the presence of the static asymmetric couplings γ_i and the mode coupling f_{\perp} an imaginary part of w_{\perp} is produced even if one starts with a zero initial value. Starting with a typical set of initial values, i.e., $w_{\parallel}(l_0) = 0.3$, $w'_{\perp}(l_0) = 0.6$, $s(l_0) = 0.5$, and $f_{\perp}(l_0) = 0.4$ at the flow parameter value $\ln l_0 = -1$, the

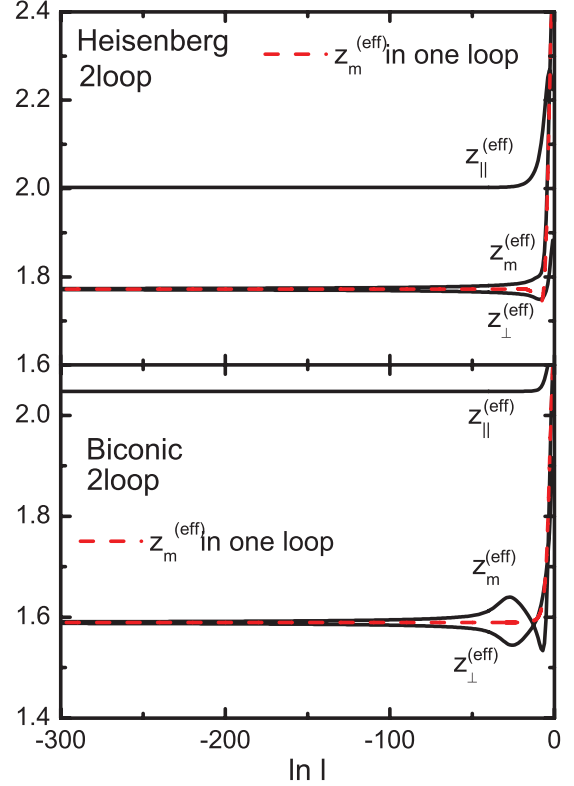


FIG. 4. (Color online) Effective dynamic exponents in the background using the flow equations (64) and (66) in two-loop order in $d = 3$ in the complete dynamical parameter space (full lines). For comparison the effective dynamic exponent $z_m^{(\text{eff})}$ in one-loop order is shown (dashed line).

effective exponents in the complete parameter space have been calculated in $d = 3$. The result is presented in Fig. 4 for both static fixed points, where the solid lines are the results of the two-loop calculation, and the dashed line is a result of a complete (flow and effective exponent) one-loop calculation. However, the static FP values from Table II have been used also in the dynamic one-loop flow. There it seems that in two-loop order the same results as in the one loop calculation are obtained. $z_{\perp}^{(\text{eff})}$ and $z_m^{(\text{eff})}$ are getting close together (solid lines) for flow parameters $l < e^{-100}$ and seem to coincide even numerically with the corresponding results in one-loop order (dashed line). This is the type of weak scaling in one-loop order, which also can be seen from Fig. 1 and in qualitative contradiction to the discussion in the previous sections (see Fig. 3). But the examination of the flow of the dynamic parameters reveals a fundamental difference between the one- and two-loop calculation. In one-loop order the dynamic parameters w'_{\perp} , s , w_{\parallel} , and f_{\perp} merge to the FP values when the effective exponents turn over in their constant asymptotic values, which is presented in Fig. 2. This happens in the region about $l < e^{-15}$ and the dynamic parameters stay constant for all lower flow parameter values. In two-loop order the situation is different. Although the two-loop results for the effective exponents look like one has reached the asymptotic region (the exponents seem to be constant), the dynamic parameters in contrast are far from their asymptotic FP values. This is presented in Fig. 5. The parameters w'_{\perp} and s are

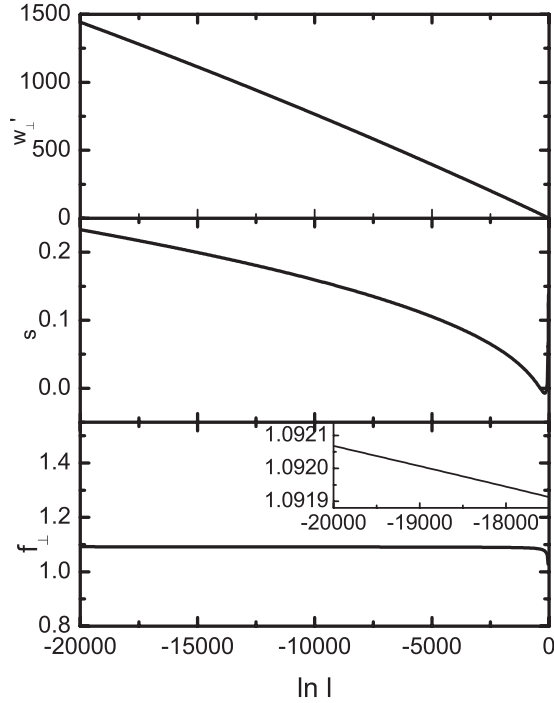


FIG. 5. Flow of the parameters w'_\perp , s , and f_\perp in the full parameter space.

still increasing and obviously have not reached a FP value. At the first glance the flow of f_\perp seems to have reached a FP value (see lowest plot in Fig. 5). But a closer examination shows that this is not the case. f_\perp is constantly increasing with a very small slope, as can be seen from the inserted small figure, where both axes have been enlarged. Actually the set of two-loop β functions does not have a zero for finite w_\perp and w_\parallel , and therefore no FP exists in the parameter region of Fig. 5. Thus the effective exponents in two-loop order in Fig. 4 show only a pseudo-asymptotic behavior completely different from real asymptotic behavior (there $z_\perp^{(\text{eff})}$ and $z_\parallel^{(\text{eff})}$ have to be equal) discussed in Sec. XC (see Fig. 3). Even if one draws the x axis in Fig. 4 down to $\ln l = -20000$, as done for the flow in Fig. 5, the picture remains to be the same, that is, the effective exponents seem to be constant, with the exception that the background behavior is not longer visible because the region is too small. Also if one changes initial conditions of the parameters the qualitative result remains the same. The different flows merge within a region of $\ln l = -150$ to the same result.

In order to get some insight how this pseudo-asymptotic behavior is possible, in Fig. 6 the relative slopes

$$\frac{1}{\alpha_i} \frac{d\alpha_i}{d \ln l} = \frac{\beta_{\alpha_i}}{\alpha_i} \quad (138)$$

for the parameters α_i chosen to be w'_\perp and f_\perp have been calculated. One can see that the relative changes in these parameters drop to very small values. As a first consequence one has to calculate down to extremely small flow parameter values $\ln l < -10^8$ where one can expect to leave the pseudo-asymptotic region. But although the β functions cannot be zero in the considered parameter range, they may reach values

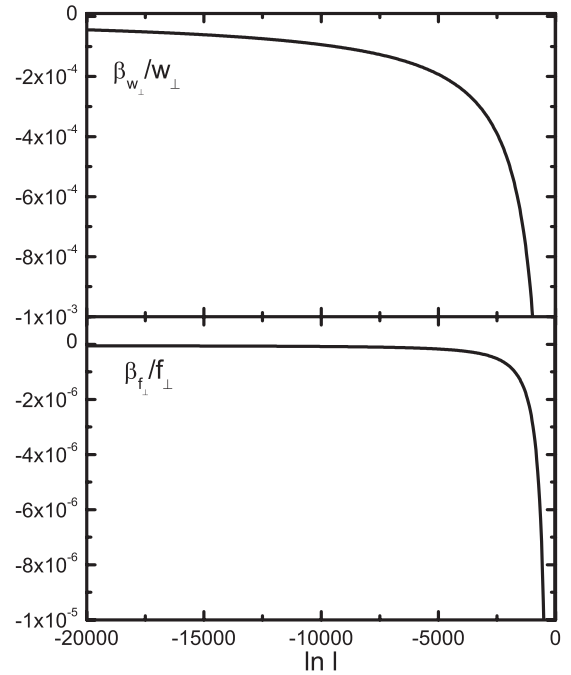


FIG. 6. Relative slope of the parameters w'_\perp and f_\perp in the full parameter space.

which are so small that they cannot longer be separated numerically from zero. This means that coming from the background it is impossible to pass the pseudo-asymptotic region numerically into the real asymptotic region. This is the reason why in the previous section the flow has been started in an asymptotic subspace.

Due to the presence of logarithmic terms in the time-scale ratio v the FP value of v has to be finite. As follows from Table IV via Eq. (122) it turns out to be very small, leading to very large (negative) values of $\ln v$. So one expects that the $\ln v$ terms begin to dominate ζ_{Γ_\perp} in a certain region of $\ln l$ near the asymptotics. Making the $\ln v$ terms explicit one may rewrite ζ_{Γ_\perp} , given in Eq. (70), as

$$\begin{aligned} \zeta_{\Gamma_\perp} = & -\frac{1}{2} \frac{\gamma_\parallel D_\perp}{1 + w_\perp} \left(\frac{u_\times}{3} + \frac{1}{2} \frac{\gamma_\parallel D_\perp}{1 + w_\perp} \right) \ln v \\ & - \frac{u_\times^2}{36} \ln v + \text{remaining terms.} \end{aligned} \quad (139)$$

Inserting Eq. (122), the essential term is the real part V' of the prefactor of $\ln q$. One obtains

$$\zeta_{\Gamma_\perp} = V' \ln q + \text{remaining terms.} \quad (140)$$

The prefactor V' is

$$V' = - \left[\frac{u_\times^2}{36} + \frac{1}{2} \gamma_\parallel A \left(\frac{u_\times}{3} + \frac{1}{2} \gamma_\parallel A \right) - \frac{1}{4} \gamma_\parallel^2 B^2 \right] \quad (141)$$

with

$$A = \frac{w'_\perp [(1 + w'_\perp + w'_\perp s^2) \gamma_\perp - sF]}{(1 + w'_\perp)^2 + (w'_\perp s)^2}, \quad (142)$$

$$B = \frac{w'_\perp s \gamma_\perp - (1 + w'_\perp)F}{(1 + w'_\perp)^2 + (w'_\perp s)^2}. \quad (143)$$

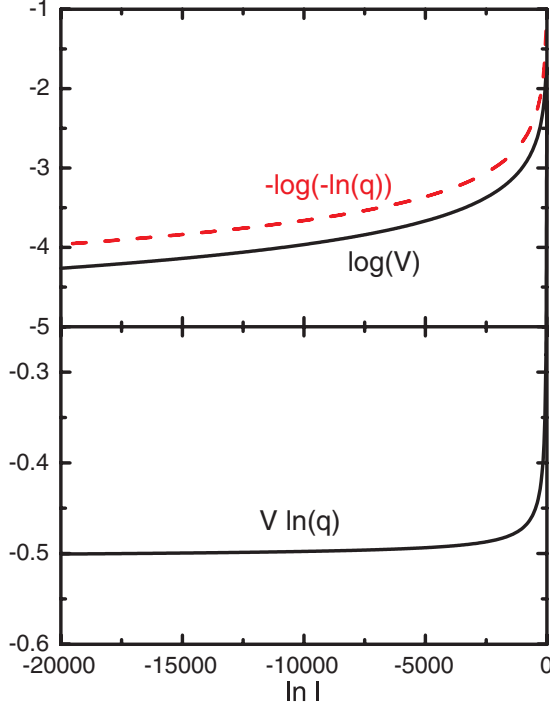


FIG. 7. (Color online) Contribution of the $V' \ln q$ term in Eq. (140) (lower figure). It is of the same magnitude as the other terms in the ζ function. V' and $\ln q$ have the same behavior with opposite exponents. This is demonstrated in the upper figure, where the decadic logarithm of V' (solid curve) and the negative decadic logarithm of $-\ln q$ have been drawn (dashed curves).

In Fig. 7 the behavior of the $\ln q$ contributions to $\zeta_{\Gamma_{\perp}}$ at the biconical FP is presented. Although the $\ln q$ term already reaches very large negative values (q is very small), as expected, this is compensated by the prefactor V' , which has very small values in the considered region. In the upper part of Fig. 7 the decadic logarithm of V' and $-\ln q$ have been plotted. Both curves show a similar behavior and a small difference. In the lower part $V' \ln q$ is calculated from (141)–(143). As a consequence of the results in the upper part of the figure the numerical values are about -0.5 , and one can see that the term is far from being the leading one. There are other contributions to $\zeta_{\Gamma_{\perp}}$ that have the same magnitude. Thus the ζ function is not in the asymptotic region, as has been also indicated by the flow in Fig. 5.

Thus one expects in the experimentally accessible region nonuniversal effective dynamical critical behavior. This is described in the crossover region to the background by the flow equations together with a suitable matching condition related to the temperature distance, the wave vector modulus, etc. The initial conditions have to be found by comparison with experiment.

XII. CONCLUSION

Our two-loop calculation for the dynamics at the multicritical point in anisotropic antiferromagnets in an external magnetic field leads to a FP where the OPs characterizing the parallel and perpendicular ordering with respect to the external

field scale in the same way (strong dynamic scaling). This holds independent whether the Heisenberg FP or the biconical FP in statics is the stable one. The nonasymptotic analysis of the dynamic flow equations show that due to cancellation effects the critical behavior is described, in distances from the critical point accessible to experiments, by the critical behavior qualitatively found in one-loop order. That means the time scales of the two OP components become almost constant in a so-called pseudo-asymptotic region and scale differently.

So far we have not included the nonasymptotic flow of the static parameters, which are expected to lead to minor deviations from the overall picture. Another item would be the study of the decoupled FP since in the nonasymptotic region the OPs remain statically and dynamically coupled, and the behavior depends on the stability exponents how fast these effects decay. This in turn depends on the distance of the system in dimensional space and the space of the OP components from the stability border line to other FPs than the decoupled FP (see Fig. 1 in paper I).

The numerical results presented in this series of papers have been calculated for dimension $d = 3$. One might speculate that the peculiar behavior found is specific to the dimension of the physical space rather than to the multicritical character of the specific point. This aspect was out of the scope of this series of papers. We note that the two critical lines meet at the multicritical point (bicritical or tetracritical) tangentially. This has been taken into account for the nonasymptotic behavior by choosing a path approaching the multicritical point without meeting one of the two critical lines [24]. The nonasymptotic behavior, in fact, is more complicated since two critical length scales are present in the system. This has to be taken into account when studying the crossover behavior in approaching one of the critical lines [25].

Only recently a bicritical point has been identified by computer simulation [26]. The corresponding FP has been identified as the Heisenberg FP, which corresponds to the type of phase diagram obtained. It seems to be difficult to look for situations where a phase diagram containing a tetracritical point is present. Even more complicated would it be to identify the dynamical characteristic of this multicritical point, where, coming from the disordered phase, two lines belonging to different dynamic universality classes meet. The dynamical universality class of the case with a $n = 1$ OP (model C) has been studied in Refs. [27,28] with different results leading to critical exponents larger than expected. The dynamical universality class of the case with a $n = 2$ OP (model F) case has been studied by computer simulations in Refs. [29,30]. The methods of these simulations might be extended in order to be used also in the case of the multicritical point studied in this paper.

ACKNOWLEDGMENTS

This work was supported by the Fonds zur Förderung der wissenschaftlichen Forschung under Project No. P19583-N20. Yu.H. acknowledges partial support from the FP7 EU IRSES project N269139 “Dynamics and Cooperative Phenomena in Complex Physical and Biological Media.” We thank one of the referees for the exceptionally critical and precise remarks that have improved the presentation.

APPENDIX A: CALCULATION OF THE DYNAMIC VERTEX FUNCTIONS OF THE OPs

In perturbation expansion up to two-loop order the functions $\hat{\Omega}_{\psi\bar{\psi}+}$, $\hat{\Gamma}_{\psi\bar{\psi}+}^{(d)}$, and $\hat{\Omega}_{\phi_{\parallel}\bar{\phi}_{\parallel}}$, which appear in Eqs. (27) and (28), can be written as

$$\hat{\Omega}_{\psi\bar{\psi}+}(\xi_{\perp}, \xi_{\parallel}, k, \omega) = 1 + \hat{\Omega}_{\psi\bar{\psi}+}^{(1L)}(\xi_{\perp}, k, \omega) + \hat{\Omega}_{\psi\bar{\psi}+}^{(2L)}(\xi_{\perp}, \xi_{\parallel}, k, \omega), \quad (\text{A1})$$

$$\begin{aligned} \hat{\Gamma}_{\psi\bar{\psi}+}^{(d)}(\xi_{\perp}, \xi_{\parallel}, k, \omega) \\ = 2[\hat{\Gamma}_{\perp} + \hat{G}_{\psi\bar{\psi}+}^{(1L)}(\xi_{\perp}, k, \omega) + \hat{G}_{\psi\bar{\psi}+}^{(2L)}(\xi_{\perp}, \xi_{\parallel}, k, \omega)], \quad (\text{A2}) \end{aligned}$$

$$\hat{\Omega}_{\phi_{\parallel}\bar{\phi}_{\parallel}}(\xi_{\perp}, \xi_{\parallel}, k, \omega) = 1 + \hat{\Omega}_{\phi_{\parallel}\bar{\phi}_{\parallel}}^{(1L)}(\xi_{\parallel}, k, \omega) + \hat{\Omega}_{\phi_{\parallel}\bar{\phi}_{\parallel}}^{(2L)}(\xi_{\perp}, \xi_{\parallel}, k, \omega). \quad (\text{A3})$$

The superscript (iL) indicates the loop order. Of course, all functions considered depend on all model parameters (couplings and kinetic coefficients), but only the independent

lengths ξ_{\perp} , ξ_{\parallel} , k , and ω will be mentioned explicitly in the following. The one-loop contributions are

$$\hat{\Omega}_{\psi\bar{\psi}+}^{(1L)}(\xi_{\perp}, k, \omega) = (\hat{\Gamma}_{\perp}\hat{\gamma}_{\perp} - i\hat{g})\hat{\gamma}_{\perp}I_{\perp}(\xi_{\perp}, k, \omega), \quad (\text{A4})$$

$$\hat{G}_{\psi\bar{\psi}+}^{(1L)}(\xi_{\perp}, k, \omega) = (\hat{\Gamma}_{\perp}\hat{\gamma}_{\perp} - i\hat{g})i\hat{g}I_{\perp}(\xi_{\parallel}, k, \omega), \quad (\text{A5})$$

$$\hat{\Omega}_{\phi_{\parallel}\bar{\phi}_{\parallel}}^{(1L)}(\xi_{\parallel}, k, \omega) = \hat{\Gamma}_{\parallel}\hat{\gamma}_{\parallel}^2I_{\parallel}(\xi_{\parallel}, k, \omega). \quad (\text{A6})$$

The one-loop integrals I_{\perp} and I_{\parallel} in Eqs. (A4)–(A6) read

$$I_{\perp}(\xi_{\perp}, k, \omega) = \int_{k'} \frac{1}{[\xi_{\perp}^{-2} + (k+k')^2](-i\omega + \alpha'_{\perp})}, \quad (\text{A7})$$

$$I_{\parallel}(\xi_{\parallel}, k, \omega) = \int_{k'} \frac{1}{[\xi_{\parallel}^{-2} + (k+k')^2](-i\omega + \alpha'_{\parallel})}. \quad (\text{A8})$$

The dynamic propagators α'_{\perp} and α'_{\parallel} are defined as

$$\alpha'_{\perp} \equiv \hat{\Gamma}_{\perp}[\xi_{\perp}^{-2} + (k+k')^2] + \hat{\lambda}k^2, \quad (\text{A9})$$

$$\alpha'_{\parallel} \equiv \hat{\Gamma}_{\parallel}[\xi_{\parallel}^{-2} + (k+k')^2] + \hat{\lambda}k^2. \quad (\text{A10})$$

The two-loop contributions to the dynamic vertex function of the orthogonal components (A1) and (A2) have the structure

$$\begin{aligned} \hat{\Omega}_{\psi\bar{\psi}+}^{(2L)}(\xi_{\perp}, \xi_{\parallel}, k, \omega) = \frac{2}{9}\hat{\Gamma}_{\perp}\hat{u}_{\perp}^2\hat{W}_{\psi\bar{\psi}+}^{(A_{\perp})}(\xi_{\perp}, k, \omega) + \frac{1}{18}\hat{\Gamma}_{\perp}\hat{u}_{\perp}^2\hat{W}_{\psi\bar{\psi}+}^{(A_{\times})}(\xi_{\perp}, \xi_{\parallel}, k, \omega) - \frac{2}{3}(2\hat{\Gamma}_{\perp}\hat{\gamma}_{\perp} - i\hat{g})\hat{u}_{\perp}\hat{F}_{\psi\bar{\psi}+}^{(T3_{\perp})}(\xi_{\perp}, k, \omega) \\ - \frac{1}{6}(2\hat{\Gamma}_{\perp}\hat{\gamma}_{\perp} - i\hat{g})\hat{u}_{\times}\hat{F}_{\psi\bar{\psi}+}^{(T3_{\times})}(\xi_{\perp}, \xi_{\parallel}, k, \omega) + (\hat{\Gamma}_{\perp}\hat{\gamma}_{\perp} - i\hat{g})\hat{\gamma}_{\perp}\hat{F}_{\psi\bar{\psi}+}(\xi_{\perp}, \xi_{\parallel}, k, \omega) \end{aligned} \quad (\text{A11})$$

and

$$\hat{G}_{\psi\bar{\psi}+}^{(2L)}(\xi_{\perp}, \xi_{\parallel}, k, \omega) = -\frac{2}{3}\hat{\Gamma}_{\perp}\hat{u}_{\perp}i\hat{g}\hat{F}_{\psi\bar{\psi}+}^{(T3_{\perp})}(\xi_{\perp}, k, \omega) - \frac{1}{6}\hat{\Gamma}_{\perp}\hat{u}_{\times}i\hat{g}\hat{F}_{\psi\bar{\psi}+}^{(T3_{\times})}(\xi_{\perp}, \xi_{\parallel}, k, \omega) + (\hat{\Gamma}_{\perp}\hat{\gamma}_{\perp} - i\hat{g})i\hat{g}\hat{F}_{\psi\bar{\psi}+}(\xi_{\perp}, \xi_{\parallel}, k, \omega). \quad (\text{A12})$$

Note that both two-loop functions differ only in terms containing the static fourth-order couplings \hat{u}_{\perp} and \hat{u}_{\times} . The remaining contributions are the same in both functions apart from a factor $\hat{\gamma}_{\perp}$ and $i\hat{g}$, respectively. The function $\hat{F}_{\psi\bar{\psi}+}$ is defined as

$$\begin{aligned} \hat{F}_{\psi\bar{\psi}+}(\xi_{\perp}, \xi_{\parallel}, k, \omega) \equiv (\hat{\Gamma}_{\perp}\hat{\gamma}_{\perp} - i\hat{g})^2\hat{F}_{\psi\bar{\psi}+}^{(T4_{\perp})}(\xi_{\perp}, k, \omega) + \hat{F}_{\psi\bar{\psi}+}^{(T5_{\perp})}(\xi_{\perp}, k, \omega) - \hat{\gamma}_{\perp}\hat{F}_{\psi\bar{\psi}+}^{(T3_{\perp})}(\xi_{\perp}, k, \omega) \\ + \frac{1}{2}[\hat{F}_{\psi\bar{\psi}+}^{(T5_{\times})}(\xi_{\perp}, \xi_{\parallel}, k, \omega) - \hat{\gamma}_{\parallel}\hat{F}_{\psi\bar{\psi}+}^{(T3_{\times})}(\xi_{\perp}, \xi_{\parallel}, k, \omega)] + \hat{F}_{\psi\bar{\psi}+}^{(T6_{\perp})}(\xi_{\perp}, k, \omega) - \hat{\gamma}_{\perp}\hat{F}_{\psi\bar{\psi}+}^{(T3_{\perp})}(\xi_{\perp}, k, \omega). \end{aligned} \quad (\text{A13})$$

The first two-loop contributions in Eq. (A11) come from the bicritical model A. The integrals $\hat{W}_{\psi\bar{\psi}+}^{(A_i)}$ are defined by

$$\hat{W}_{\psi\bar{\psi}+}^{(A_{\perp})}(\xi_{\perp}, k, \omega) = \int_{k'} \int_{k''} \frac{1}{[\xi_{\perp}^{-2} + (k+k')^2](\xi_{\perp}^{-2} + k''^2)[\xi_{\perp}^{-2} + (k'+k'')^2](-i\omega + A_{\perp\perp\perp})}, \quad (\text{A14})$$

$$\hat{W}_{\psi\bar{\psi}+}^{(A_{\times})}(\xi_{\perp}, \xi_{\parallel}, k, \omega) = \int_{k'} \int_{k''} \frac{1}{[\xi_{\perp}^{-2} + (k+k')^2](\xi_{\parallel}^{-2} + k''^2)[\xi_{\parallel}^{-2} + (k'+k'')^2](-i\omega + A_{\perp\parallel\parallel})} \quad (\text{A15})$$

with

$$A_{\perp\perp\perp} \equiv \hat{\Gamma}_{\perp}[\xi_{\perp}^{-2} + (k+k')^2] + \hat{\Gamma}_{\perp}^+[\xi_{\perp}^{-2} + k''^2] + \hat{\Gamma}_{\perp}[\xi_{\perp}^{-2} + (k'+k'')^2] \quad (\text{A16})$$

and

$$A_{\perp\parallel\parallel} \equiv \hat{\Gamma}_{\perp}[\xi_{\perp}^{-2} + (k+k')^2] + \hat{\Gamma}_{\parallel}(\xi_{\parallel}^{-2} + k''^2) + \hat{\Gamma}_{\parallel}[\xi_{\parallel}^{-2} + (k'+k'')^2]. \quad (\text{A17})$$

The further two-loop contributions in Eqs. (A11)–(A13) are marked with superscripts (Ti), which indicate the different graph topologies. The explicit expressions are

$$\hat{F}_{\psi\bar{\psi}+}^{(T3_{\perp})}(\xi_{\perp}, k, \omega) = \int_{k'} \int_{k''} \frac{1}{[\xi_{\perp}^{-2} + (k+k')^2](-i\omega + \alpha'_{\perp})(-i\omega + A_{\perp\perp\perp})} \left[\frac{\hat{\Gamma}_{\perp}\hat{\gamma}_{\perp} - i\hat{g}}{\xi_{\perp}^{-2} + k''^2} + \frac{\hat{\Gamma}_{\perp}^+\hat{\gamma}_{\perp} + i\hat{g}}{\xi_{\perp}^{-2} + (k'+k'')^2} \right], \quad (\text{A18})$$

$$\hat{F}_{\psi\bar{\psi}+}^{(T3_{\times})}(\xi_{\perp}, \xi_{\parallel}, k, \omega) = \int_{k'} \int_{k''} \frac{2\hat{\Gamma}_{\parallel}\hat{\gamma}_{\parallel}}{[\xi_{\perp}^{-2} + (k+k')^2](\xi_{\parallel}^{-2} + k''^2)(-i\omega + \alpha'_{\parallel})(-i\omega + A_{\perp\parallel\parallel})}, \quad (\text{A19})$$

$$\mathring{F}_{\psi\bar{\psi}^+}^{(T4_{\perp})}(\xi_{\perp}, k, \omega) = \int_{k'} \int_{k''} \frac{1}{[\xi_{\perp}^{-2} + (k + k' + k'')^2](-i\omega + \alpha'_{\perp})^2(-i\omega + \beta_{\perp})}, \quad (\text{A20})$$

$$\mathring{F}_{\psi\bar{\psi}^+}^{(T5_{\perp})}(\xi_{\perp}, k, \omega) = \int_{k'} \int_{k''} \frac{\mathring{\gamma}_{\perp} \mathring{\lambda} k'^2 - i\mathring{g}[(k' + k'')^2 - k'^2]}{[\xi_{\perp}^{-2} + (k + k')^2](-i\omega + \alpha'_{\perp})^2(-i\omega + A_{\perp\perp+\perp})} \left[\frac{\mathring{\Gamma}_{\perp} \mathring{\gamma}_{\perp} - i\mathring{g}}{\xi_{\perp}^{-2} + k'^2} + \frac{\mathring{\Gamma}_{\perp}^+ \mathring{\gamma}_{\perp} + i\mathring{g}}{\xi_{\perp}^{-2} + (k' + k'')^2} \right], \quad (\text{A21})$$

$$\mathring{F}_{\psi\bar{\psi}^+}^{(T5_{\times})}(\xi_{\perp}, \xi_{\parallel}, k, \omega) = \int_{k'} \int_{k''} \frac{2\mathring{\Gamma}_{\parallel} \mathring{\gamma}_{\parallel}^2 \mathring{\lambda} k'^2}{[\xi_{\perp}^{-2} + (k + k')^2](\xi_{\parallel}^{-2} + k'^2)(-i\omega + \alpha'_{\perp})^2(-i\omega + A_{\perp\parallel\parallel})}, \quad (\text{A22})$$

$$\begin{aligned} \mathring{F}_{\psi\bar{\psi}^+}^{(T6_{\perp})}(\xi_{\perp}, k, \omega) &= \int_{k'} \int_{k''} \frac{\mathring{\gamma}_{\perp} \mathring{\lambda} k'^2 + i\mathring{g}[(k + k' + k'')^2 - (k + k')^2]}{[\xi_{\perp}^{-2} + (k + k')^2](-i\omega + \alpha'_{\perp})(-i\omega + \alpha'_{\perp})(-i\omega + S_{\perp\perp+\perp})} \left[\frac{\mathring{\Gamma}_{\perp} \mathring{\gamma}_{\perp} - i\mathring{g}}{\xi_{\perp}^{-2} + (k + k' + k'')^2} + \frac{\mathring{\Gamma}_{\perp}^+ \mathring{\gamma}_{\perp} + i\mathring{g}}{\xi_{\perp}^{-2} + (k + k'')^2} \right] \\ &+ \int_{k'} \int_{k''} \frac{\mathring{\Gamma}_{\perp} \mathring{\gamma}_{\perp} - i\mathring{g}}{[\xi_{\perp}^{-2} + (k + k')^2](-i\omega + \alpha'_{\perp})(-i\omega + \beta_{\perp})} \left\{ \frac{\mathring{\Gamma}_{\perp} \mathring{\gamma}_{\perp} - i\mathring{g}}{-i\omega + \alpha'_{\perp}} + \frac{\mathring{\gamma}_{\perp}}{\xi_{\perp}^{-2} + (k + k' + k'')^2} \right. \\ &\left. + \frac{\mathring{\gamma}_{\perp} \mathring{\lambda} k'^2 + i\mathring{g}[(k + k' + k'')^2 - (k + k')^2]}{[\xi_{\perp}^{-2} + (k + k' + k'')^2](-i\omega + \alpha'_{\perp})} \right\}, \quad (\text{A23}) \end{aligned}$$

with the dynamic propagators

$$\beta_{\perp} \equiv \mathring{\Gamma}_{\perp}[\xi_{\perp}^{-2} + (k + k' + k'')^2] + \mathring{\lambda}(k'^2 + k''^2), \quad (\text{A24})$$

$$S_{\perp\perp+\perp} \equiv \mathring{\Gamma}_{\perp}[\xi_{\perp}^{-2} + (k + k')^2] + \mathring{\Gamma}_{\perp}^+[\xi_{\perp}^{-2} + (k + k' + k'')^2] + \mathring{\Gamma}_{\perp}[\xi_{\perp}^{-2} + (k + k'')^2], \quad (\text{A25})$$

which are both invariant under an interchange of k' and k'' , and $\alpha''_{\perp} \equiv \mathring{\Gamma}_{\perp}(\xi_{\perp}^{-2} + (k + k'')^2) + \mathring{\lambda}k'^2$.

The two-loop contributions to the dynamic vertex function of the parallel component (A3) have the structure

$$\begin{aligned} \mathring{\Omega}_{\phi_{\parallel}\bar{\phi}_{\parallel}}^{(2L)}(\xi_{\perp}, \xi_{\parallel}, k, \omega) &= \frac{1}{6} \mathring{\Gamma}_{\parallel} \mathring{u}_{\parallel}^2 \mathring{W}_{\phi_{\parallel}\bar{\phi}_{\parallel}}^{(A_{\parallel})}(\xi_{\parallel}, k, \omega) + \frac{1}{9} \mathring{\Gamma}_{\parallel} \mathring{u}_{\parallel}^2 \mathring{W}_{\phi_{\parallel}\bar{\phi}_{\parallel}}^{(A_{\times})}(\xi_{\perp}, \xi_{\parallel}, k, \omega) - \mathring{\Gamma}_{\parallel} \mathring{u}_{\parallel} \mathring{\gamma}_{\parallel} \mathring{F}_{\phi_{\parallel}\bar{\phi}_{\parallel}}^{(T3_{\parallel})}(\xi_{\parallel}, k, \omega) \\ &- \frac{2}{3} \mathring{\Gamma}_{\parallel} \mathring{u}_{\parallel} \mathring{\gamma}_{\parallel} \mathring{F}_{\phi_{\parallel}\bar{\phi}_{\parallel}}^{(T3_{\times})}(\xi_{\perp}, \xi_{\parallel}, k, \omega) + \mathring{\Gamma}_{\parallel} \mathring{\gamma}_{\parallel}^2 \mathring{F}_{\phi_{\parallel}\bar{\phi}_{\parallel}}(\xi_{\perp}, \xi_{\parallel}, k, \omega). \quad (\text{A26}) \end{aligned}$$

The function $\mathring{F}_{\phi_{\parallel}\bar{\phi}_{\parallel}}$ is defined as

$$\begin{aligned} \mathring{F}_{\phi_{\parallel}\bar{\phi}_{\parallel}}(\xi_{\perp}, \xi_{\parallel}, k, \omega) &\equiv \mathring{\Gamma}_{\parallel}^2 \mathring{\gamma}_{\parallel}^2 \mathring{F}_{\phi_{\parallel}\bar{\phi}_{\parallel}}^{(T4_{\parallel})}(\xi_{\parallel}, k, \omega) + \frac{1}{2} (\mathring{F}_{\phi_{\parallel}\bar{\phi}_{\parallel}}^{(T5_{\parallel})}(\xi_{\parallel}, k, \omega) - \mathring{\gamma}_{\parallel} \mathring{F}_{\phi_{\parallel}\bar{\phi}_{\parallel}}^{(T3_{\parallel})}(\xi_{\parallel}, k, \omega)) + \mathring{F}_{\phi_{\parallel}\bar{\phi}_{\parallel}}^{(T5_{\times})}(\xi_{\perp}, \xi_{\parallel}, k, \omega) \\ &- \mathring{\gamma}_{\perp} \mathring{F}_{\phi_{\parallel}\bar{\phi}_{\parallel}}^{(T3_{\times})}(\xi_{\perp}, \xi_{\parallel}, k, \omega) + \mathring{F}_{\phi_{\parallel}\bar{\phi}_{\parallel}}^{(T6_{\parallel})}(\xi_{\parallel}, k, \omega) - \mathring{\gamma}_{\parallel} \mathring{F}_{\phi_{\parallel}\bar{\phi}_{\parallel}}^{(T3_{\parallel})}(\xi_{\parallel}, k, \omega). \quad (\text{A27}) \end{aligned}$$

The integrals $\mathring{W}_{\phi_{\parallel}\bar{\phi}_{\parallel}}^{(A_i)}$ in the two-loop contributions from the bicritical model A are

$$\mathring{W}_{\phi_{\parallel}\bar{\phi}_{\parallel}}^{(A_{\parallel})}(\xi_{\parallel}, k, \omega) = \int_{k'} \int_{k''} \frac{1}{[\xi_{\parallel}^{-2} + (k + k')^2](\xi_{\parallel}^{-2} + k'^2)[\xi_{\parallel}^{-2} + (k' + k'')^2](-i\omega + A_{\parallel\parallel\parallel})}, \quad (\text{A28})$$

$$\mathring{W}_{\phi_{\parallel}\bar{\phi}_{\parallel}}^{(A_{\times})}(\xi_{\perp}, \xi_{\parallel}, k, \omega) = \int_{k'} \int_{k''} \frac{1}{[\xi_{\parallel}^{-2} + (k + k')^2](\xi_{\perp}^{-2} + k'^2)[\xi_{\perp}^{-2} + (k' + k'')^2](-i\omega + A_{\parallel\perp+\perp})} \quad (\text{A29})$$

with the propagators

$$A_{\parallel\parallel\parallel} \equiv \mathring{\Gamma}_{\parallel}[\xi_{\parallel}^{-2} + (k + k')^2] + \mathring{\Gamma}_{\parallel}(\xi_{\parallel}^{-2} + k'^2) + \mathring{\Gamma}_{\parallel}[\xi_{\parallel}^{-2} + (k' + k'')^2], \quad (\text{A30})$$

and

$$A_{\parallel\perp+\perp} \equiv \mathring{\Gamma}_{\parallel}[\xi_{\parallel}^{-2} + (k + k')^2] + \mathring{\Gamma}_{\perp}^+(\xi_{\perp}^{-2} + k'^2) + \mathring{\Gamma}_{\perp}[\xi_{\perp}^{-2} + (k' + k'')^2]. \quad (\text{A31})$$

The remaining two-loop contributions in Eqs. (A26) and (A27) are

$$\mathring{F}_{\phi_{\parallel}\bar{\phi}_{\parallel}}^{(T3_{\parallel})}(\xi_{\parallel}, k, \omega) = \int_{k'} \int_{k''} \frac{2\mathring{\Gamma}_{\parallel} \mathring{\gamma}_{\parallel}}{[\xi_{\parallel}^{-2} + (k + k')^2](\xi_{\parallel}^{-2} + k'^2)(-i\omega + \alpha'_{\parallel})(-i\omega + A_{\parallel\parallel\parallel})}, \quad (\text{A32})$$

$$\mathring{F}_{\phi_{\parallel}\bar{\phi}_{\parallel}}^{(T3_{\times})}(\xi_{\perp}, \xi_{\parallel}, k, \omega) = \int_{k'} \int_{k''} \frac{1}{[\xi_{\parallel}^{-2} + (k + k')^2](-i\omega + \alpha'_{\parallel})(-i\omega + A_{\parallel\perp+\perp})} \left[\frac{\mathring{\Gamma}_{\perp} \mathring{\gamma}_{\perp} - i\mathring{g}}{\xi_{\perp}^{-2} + k'^2} + \frac{\mathring{\Gamma}_{\perp}^+ \mathring{\gamma}_{\perp} + i\mathring{g}}{\xi_{\perp}^{-2} + (k' + k'')^2} \right], \quad (\text{A33})$$

$$\mathring{F}_{\phi_{\parallel}\tilde{\phi}_{\parallel}}^{(T4_{\parallel})}(\xi_{\parallel}, k, \omega) = \int_{k'} \int_{k''} \frac{1}{[\xi_{\parallel}^{-2} + (k+k'+k'')^2](-i\omega + \alpha'_{\parallel})^2(-i\omega + \beta_{\parallel})}, \quad (\text{A34})$$

$$\mathring{F}_{\phi_{\parallel}\tilde{\phi}_{\parallel}}^{(T5_{\parallel})}(\xi_{\parallel}, k, \omega) = \int_{k'} \int_{k''} \frac{2\mathring{\Gamma}_{\parallel}\mathring{\gamma}_{\parallel}^2\mathring{\lambda}k'^2}{[\xi_{\parallel}^{-2} + (k+k')^2](\xi_{\parallel}^{-2} + k''^2)(-i\omega + \alpha'_{\parallel})^2(-i\omega + A_{\parallel\parallel})}, \quad (\text{A35})$$

$$\mathring{F}_{\phi_{\parallel}\tilde{\phi}_{\parallel}}^{(T5_{\perp})}(\xi_{\perp}, \xi_{\parallel}, k, \omega) = \int_{k'} \int_{k''} \frac{\mathring{\gamma}_{\perp}\mathring{\lambda}k'^2 - i\mathring{g}[(k'+k'')^2 - k''^2]}{[\xi_{\parallel}^{-2} + (k+k')^2](-i\omega + \alpha'_{\parallel})^2(-i\omega + A_{\parallel\perp+\perp})} \left[\frac{\mathring{\Gamma}_{\perp}\mathring{\gamma}_{\perp} - i\mathring{g}}{\xi_{\perp}^{-2} + k''^2} + \frac{\mathring{\Gamma}_{\perp}^+\mathring{\gamma}_{\perp} + i\mathring{g}}{\xi_{\perp}^{-2} + (k'+k'')^2} \right], \quad (\text{A36})$$

$$\begin{aligned} \mathring{F}_{\phi_{\parallel}\tilde{\phi}_{\parallel}}^{(T6_{\parallel})}(\xi_{\parallel}, k, \omega) &= \int_{k'} \int_{k''} \frac{\mathring{\Gamma}_{\parallel}\mathring{\gamma}_{\parallel}^2\mathring{\lambda}k''^2}{[\xi_{\parallel}^{-2} + (k+k')^2](-i\omega + \alpha'_{\parallel})(-i\omega + \alpha''_{\parallel})(-i\omega + S_{\parallel\parallel\parallel})} \left[\frac{1}{\xi_{\parallel}^{-2} + (k+k'+k'')^2} + \frac{1}{\xi_{\parallel}^{-2} + (k+k'')^2} \right] \\ &+ \int_{k'} \int_{k''} \frac{\mathring{\Gamma}_{\parallel}\mathring{\gamma}_{\parallel}^2}{[\xi_{\parallel}^{-2} + (k+k')^2](-i\omega + \alpha''_{\parallel})(-i\omega + \beta_{\parallel})} \left[\frac{\mathring{\Gamma}_{\parallel}}{-i\omega + \alpha'_{\parallel}} + \frac{1}{\xi_{\parallel}^{-2} + (k+k'+k'')^2} \left(1 + \frac{\mathring{\lambda}k''^2}{-i\omega + \alpha''_{\parallel}} \right) \right]. \end{aligned} \quad (\text{A37})$$

The additional dynamic propagators are

$$S_{\parallel\parallel\parallel} \equiv \mathring{\Gamma}_{\parallel}[\xi_{\parallel}^{-2} + (k+k')^2] + \mathring{\Gamma}_{\parallel}[\xi_{\parallel}^{-2} + (k+k'+k'')^2] + \mathring{\Gamma}_{\parallel}[\xi_{\parallel}^{-2} + (k+k'')^2]$$

and

$$\alpha''_{\parallel} \equiv \mathring{\Gamma}_{\parallel}[\xi_{\parallel}^{-2} + (k+k'')^2] + \mathring{\lambda}k''^2, \quad \beta_{\parallel} \equiv \mathring{\Gamma}_{\parallel}[\xi_{\parallel}^{-2} + (k+k'+k'')^2] + \mathring{\lambda}(k^2 + k''^2). \quad (\text{A38})$$

The integrals contained in Eqs. (A14)–(A23) and (A28)–(A37) are of the same type as already has been presented in Ref. [31] [see Eqs. (A19)–(A26) in the Appendix therein]. The ε poles of these integrals can be found in Eqs. (C2)–(C19) of the same reference.

APPENDIX B: DYNAMIC Z FACTORS IN TWO-LOOP ORDER

Within the minimal subtraction scheme of the renormalization group calculation one has to collect in two-loop order the pole terms of order $1/\varepsilon^2$ and $1/\varepsilon$ in the functions $\mathring{\Omega}_{\psi\tilde{\psi}^+}$ and $\mathring{\Gamma}_{\psi\tilde{\psi}^+}^{(d)}$ in Eq. (27). The resulting dynamic renormalization factors are

$$\begin{aligned} Z_{\tilde{\psi}^*}^{1/2} &= 1 - \frac{1}{\varepsilon} \frac{\gamma_{\perp} D_{\perp}}{1 + w_{\perp}} - \frac{1}{\varepsilon} \left[\frac{u_{\perp}^2}{18} \left(L_0 + x_1 L_1 - \frac{1}{4} \right) + \frac{u_{\times}^2}{72} \left(L_{\perp}^{(\times)} - \frac{1}{4} \right) \right] \\ &+ \frac{1}{4\varepsilon} \left\{ \frac{2}{3} \frac{u_{\perp}(w_{\perp}\gamma_{\perp} + D_{\perp})}{w_{\perp}(1 + w_{\perp})} A_{\perp} + \frac{\gamma_{\perp} D_{\perp}}{w_{\perp}(1 + w_{\perp})^2} B_{\perp} + \frac{\gamma_{\parallel}}{2(1 + w_{\perp})} \left[\frac{u_{\times}}{3} (w_{\perp}\gamma_{\perp} + D_{\perp}) + \frac{w_{\perp}\gamma_{\perp}\gamma_{\parallel} D_{\perp}}{1 + w_{\perp}} \right] X_{\perp} \right\} \\ &+ \frac{1}{2\varepsilon^2} \left\{ - \frac{w_{\perp}\gamma_{\perp} + D_{\perp}}{1 + w_{\perp}} \left(\frac{2}{3} u_{\perp}\gamma_{\perp} + \frac{u_{\times}}{6} \gamma_{\parallel} \right) + \frac{\gamma_{\perp} D_{\perp}}{(1 + w_{\perp})^2} \left[\frac{D_{\perp}^2}{1 + w_{\perp}} - w_{\perp}^2 \left(\gamma_{\perp}^2 + \frac{\gamma_{\parallel}^2}{2} \right) - \frac{f_{\perp}^2}{2} \right] \right\}, \end{aligned} \quad (\text{B1})$$

$$\begin{aligned} Z_{\Gamma_{\perp}}^{(d)} &= 1 - \frac{1}{\varepsilon} \frac{iF D_{\perp}}{w_{\perp}(1 + w_{\perp})} + \frac{1}{4\varepsilon} \left[\frac{2}{3} \frac{u_{\perp} iF}{w_{\perp}(1 + w_{\perp})} A_{\perp} + \frac{iF D_{\perp}}{w_{\perp}^2(1 + w_{\perp})^2} B_{\perp} + \frac{\gamma_{\parallel} iF}{2(1 + w_{\perp})} \left(\frac{u_{\times}}{3} + \frac{\gamma_{\parallel} D_{\perp}}{1 + w_{\perp}} \right) X_{\perp} \right] \\ &+ \frac{1}{2\varepsilon^2} \left\{ - \frac{iF}{1 + w_{\perp}} \left(\frac{2}{3} u_{\perp}\gamma_{\perp} + \frac{u_{\times}}{6} \gamma_{\parallel} \right) + \frac{iF D_{\perp}}{w_{\perp}(1 + w_{\perp})^2} \left[\frac{D_{\perp}^2}{1 + w_{\perp}} - w_{\perp}^2 \left(\gamma_{\perp}^2 + \frac{\gamma_{\parallel}^2}{2} \right) - \frac{f_{\perp}^2}{2} \right] \right\}. \end{aligned} \quad (\text{B2})$$

The coupling D_{\perp} and the functions A_{\perp} , B_{\perp} , X_{\perp} and $L_{\perp}^{(\times)}$ are defined in Eqs. (71)–(74), (79). The pole terms of the function $\mathring{\Gamma}_{\phi_{\parallel}\tilde{\phi}_{\parallel}^+}^{(d)}$ are collected in the renormalization factor

$$\begin{aligned} Z_{\Gamma_{\parallel}} &= 1 + \frac{1}{\varepsilon} \frac{w_{\parallel}\gamma_{\parallel}^2}{1 + w_{\parallel}} + \frac{1}{\varepsilon} \left[\frac{u_{\parallel}^2}{8} \left(\ln \frac{4}{3} - \frac{1}{6} \right) + \frac{u_{\times}^2}{36} \left(L_{\parallel}^{(\times)} - \frac{1}{2} \right) \right] \\ &- \frac{1}{4\varepsilon} \left\{ \frac{w_{\parallel}\gamma_{\parallel}^2}{1 + w_{\parallel}} u_{\parallel} \left(1 - 3 \ln \frac{4}{3} \right) + \left(\frac{w_{\parallel}\gamma_{\parallel}^2}{1 + w_{\parallel}} \right)^2 \left[\frac{1}{2} \left(1 - 9 \ln \frac{4}{3} \right) - \frac{w_{\parallel}}{1 + w_{\parallel}} - \frac{1 + 2w_{\parallel}}{1 + w_{\parallel}} \ln \frac{(1 + w_{\parallel})^2}{1 + 2w_{\parallel}} \right] \right\} \end{aligned}$$

$$\begin{aligned}
& + \left(\frac{2}{3} u_{\times} + \frac{w_{\parallel} \gamma_{\parallel}}{1 + w_{\parallel}} \gamma_{\perp} \right) \operatorname{Re} \left(\frac{T_1}{w'_{\perp}} \right) - \frac{\gamma_{\parallel} F}{2w'_{\perp}(1 + w_{\parallel})} \operatorname{Im} \left(\frac{T_2}{w'_{\perp}} \right) \Big\} \\
& + \frac{1}{2\varepsilon^2} \frac{w_{\parallel} \gamma_{\parallel}}{1 + w_{\parallel}} \left\{ u_{\parallel} \gamma_{\parallel} + \frac{2}{3} u_{\times} \gamma_{\perp} + \frac{\gamma_{\parallel}}{1 + w_{\parallel}} \left[w_{\parallel} \gamma_{\parallel}^2 \left(\frac{1}{2} - \frac{w_{\parallel}}{1 + w_{\parallel}} \right) + w_{\parallel} \gamma_{\perp}^2 + \frac{f_{\perp}^2}{2} \right] + \frac{2w_{\parallel} \gamma_{\parallel}^3}{1 + w_{\parallel}} \right\}. \quad (\text{B3})
\end{aligned}$$

The functions T_1 , T_2 , and $L_{\parallel}^{(\times)}$ have been introduced in Eqs. (81)–(84).

The renormalization factor Z_{λ} is identical to the one of model F [22] with all parameters of the perpendicular subsystem. With \mathcal{Q} defined in (88), one gets

$$Z_{\lambda}^{(d)} = 1 - \frac{1}{\varepsilon} \frac{f_{\perp}^2}{2} \left\{ 1 + \frac{\mathcal{Q}}{2} - \frac{1}{4\varepsilon} \frac{1}{w'_{\perp}} \left[\frac{D_{\perp}^2}{1 + w_{\perp}} + \frac{D_{\perp}^{+2}}{1 + w_{\perp}^+} \right] \right\} \quad (\text{B4})$$

-
- [1] J. M. Kosterlitz, D. Nelson, and M. E. Fisher, *Phys. Rev. B* **13**, 412 (1976).
- [2] R. Folk, Yu. Holovatch, and G. Moser, *Phys. Rev. E* **78**, 041124 (2008); henceforth called paper I.
- [3] R. Folk and G. Moser, *J. Phys. A: Math. Gen.* **39**, R207 (2006).
- [4] B. D. Josephson, *Phys. Lett.* **21**, 608 (1966).
- [5] B. I. Halperin and P. C. Hohenberg, *Phys. Rev.* **177**, 952 (1969).
- [6] V. Dohm and H.-K. Janssen, *Phys. Rev. Lett.* **39**, 946 (1977); *J. Appl. Phys.* **49**, 1347 (1978).
- [7] V. Dohm, in *Multicritical Phenomena* (Plenum, New York, 1983), p. 81.
- [8] V. Dohm, Report of the Kernforschungsanlage Jülich Nr. 1578 (1979).
- [9] R. Folk and G. Moser, *Phys. Rev. E* **69**, 036101 (2004).
- [10] V. Dohm, *Phys. Rev. B* **44**, 2697 (1991); **73**, 099901(E) (2006).
- [11] R. Folk, Yu. Holovatch, and G. Moser, *Phys. Rev. E* **79**, 031109 (2009); henceforth called paper III.
- [12] R. Folk, Yu. Holovatch, and G. Moser, *Phys. Rev. E* **78**, 041125 (2008); henceforth called paper II.
- [13] see e.g., J. Zinn-Justin, *Quantum Field Theory and Critical Phenomena (International Series of Monographs on Physics, 92)* (Oxford University Press, Oxford, 1996); H. Kleinert and V. Schulte-Frohlinde, *Critical Properties of ϕ^4 -Theories* (World Scientific, Singapore, 2001); A. N. Vasil'ev, *The Field Theoretic Renormalization Group in Critical Behavior Theory and Stochastic Dynamics* (Chapman Hall/CRC, New York, 2004).
- [14] R. Folk, Yu. Holovatch, and G. Moser, *Europhys. Lett.* **91**, 46002 (2010).
- [15] D. L. Huber, *Phys. Lett. A* **49**, 345 (1974).
- [16] D. L. Huber and R. Raghavan, *Phys. Rev. B* **14**, 4068 (1976).
- [17] R. Freedman and F. Mazenko, *Phys. Rev. B* **13**, 4967 (1976); B. I. Halperin, P. C. Hohenberg, and E. D. Siggia, *Phys. Rev. Lett.* **32**, 1289 (1974).
- [18] R. Bausch, H. K. Janssen, and H. Wagner, *Z. Phys. B* **24**, 113 (1976).
- [19] R. Folk and G. Moser, *Phys. Rev. Lett.* **89**, 125301 (2002); **93**, 229902(E) (2004).
- [20] R. Schloms and V. Dohm, *Europhys. Lett.* **3**, 413 (1987); *Nucl. Phys. B* **328**, 639 (1989).
- [21] V. Dohm, *Z. Phys. B* **60**, 61 (1985).
- [22] V. Dohm, *Z. Phys. B* **61**, 193 (1985).
- [23] We use for the values of the static exponents ϕ/ν its expression defined by the FP values of the asymmetric couplings via $2\phi/\nu - 3 = \gamma_{\perp}^{*2} + \gamma_{\parallel}^{*2}/2$.
- [24] For specialists we note that this condition is represented by Eq. (73) in paper I.
- [25] D. J. Amit and Y. Y. Goldschmidt, *Ann. Physics* **114**, 356 (1978).
- [26] W. Selke, *Phys. Rev. E* **83**, 042102 (2011).
- [27] P. Sen, S. Dasgupta, and D. Stauffer, *Eur. Phys. J. B* **1**, 107 (1999).
- [28] D. Stauffer, *J. Mod. Phys. C* **8**, 1263 (1998).
- [29] M. Krech and D. P. Landau, *Phys. Rev. B* **60**, 3375 (1999).
- [30] D. P. Landau and M. Krech, *J. Phys. Condens. Matter* **11**, R179 (1999).
- [31] R. Folk and G. Moser, *Phys. Rev. E* **73**, 016141 (2006).